Fuel cycle modelling of open cycle thorium-fuelled nuclear energy systems

Annals of Nuclear Energy 69 (2014) 314–330

Contents lists available at ScienceDirect

Annals of Nuclear Energy

journal homepage: www.elsevier.com/locate/anucene

Fuel cycle modelling of open cycle thorium-fuelled nuclear energy systems

S.F. Ashley [a,*], B.A. Lindley [a], G.T. Parks [a], W.J. Nuttall [b], R. Gregg [c], K.W. Hesketh [c], U. Kannan [d], P.D. Krishnani [d], B. Singh [d], A. Thakur [d], M. Cowper [e,1], A. Talamo [f]

[a] Department of Engineering, University of Cambridge, Cambridge CB2 1PZ, United Kingdom
[b] Department of Engineering and Innovation, The Open University, Milton Keynes MK7 6AA, United Kingdom
[c] UK National Nuclear Laboratory, Springfields, Preston PR4 0XJ, United Kingdom
[d] Reactor Physics Design Division, Bhabha Atomic Research Centre, Trombay, Mumbai 400085, India
[e] NTEC, Department of Physics, University of Liverpool, The Oliver Lodge Laboratory, Oxford Street, Liverpool L69 7ZE, United Kingdom
[f] Nuclear Engineering Division, Argonne National Laboratory, 9700 South Cass Avenue, Argonne, IL 60439, USA

ARTICLE INFO

Article history:
Received 12 August 2013
Received in revised form 22 January 2014
Accepted 28 January 2014
Available online 18 March 2014

Keywords:
Thorium
Nuclear energy
Fuel cycle modelling
Open nuclear fuel cycle
Proliferation resistance

ABSTRACT

In this study, we have sought to determine the advantages, disadvantages, and viability of open cycle thorium–uranium-fuelled (Th–U-fuelled) nuclear energy systems. This has been done by assessing three such systems, each of which requires uranium enriched to ~20% ^{235}U, in comparison to a reference uranium-fuelled (U-fuelled) system over various performance indicators, spanning material flows, waste composition, economics, and proliferation resistance. The values of these indicators were determined using the UK National Nuclear Laboratory's fuel cycle modelling code ORION. This code required the results of lattice-physics calculations to model the neutronics of each nuclear energy system, and these were obtained using various nuclear reactor physics codes and burn-up routines. In summary, all three Th–U-fuelled nuclear energy systems required more separative work capacity than the equivalent benchmark U-fuelled system, with larger levelised fuel cycle costs and larger levelised cost of electricity. Although a reduction of ~6% in the required uranium ore per kWh was seen for one of the Th–U-fuelled systems compared to the reference U-fuelled system, the other two Th–U-fuelled systems required more uranium ore per kWh than the reference. Negligible advantages and disadvantages were observed for the amount and the properties of the spent nuclear fuel (SNF) generated by the systems considered. Two of the Th–U-fuelled systems showed some benefit in terms of proliferation resistance of the SNF generated. Overall, it appears that there is little merit in incorporating thorium into nuclear energy systems operating with open nuclear fuel cycles.

1. Introduction

At the time of writing, the majority of the world's electricity generating nuclear energy systems are fuelled with low-enriched uranium (LEU) and operate on open nuclear fuel cycles, where the U-based fuel is used only once with a view to being directly disposed of after a cooling period, i.e. the spent nuclear fuel (SNF) is neither reprocessed nor reused. Uranium reserves are typically graded in terms of their economic viability (United Nations, 2007). According to the most recent OECD report (OECD-NEA Report, 2012) there are 3.08×10^6 tonnes of uranium recoverable for less than US$80/kgU, 5.33×10^6 tonnes of uranium recoverable for less than US$130/kgU, and 7.10×10^6 tonnes of uranium recoverable for less than US$260/kgU. Present estimates for global uranium reserves, including unconventional resources such as coal ash and phosphates (but excluding seawater), range from 1.92×10^7 tonnes (Tulsidas, 2011) to 3.93×10^7 tonnes (Romanello et al., 2012). At 2012 consumption rates of 67,990 tonnes of uranium per year (World Nuclear Association, 2013), this global supply would last 78.3 years for ore recoverable for under US$130/kgU and 578 years for assumed global uranium reserves of 3.93×10^7 tonnes. The work of Romanello et al. (2012) suggests that a burgeoning demand for electricity across the world will yield a significant increase in nuclear energy capacity, and correspondingly a significant increase in uranium consumption. Their predic-

* Corresponding author. Present address: Department of Engineering and Innovation, The Open University, Milton Keynes MK7 6AA, United Kingdom. Tel.: +44 1908 858358.
E-mail address: sfa24@cam.ac.uk (S.F. Ashley).
[1] Present address: Applied Modelling & Computational Group, Department of Earth Science and Engineering, Imperial College London, London SW7 2AZ, United Kingdom.

http://dx.doi.org/10.1016/j.anucene.2014.01.042
0306-4549

tions (assuming only open nuclear fuel cycles) suggest that the reserve of ore recoverable for under US$130/kgU would be exhausted by ~2060 and a total reserve of 3.93×10^7 tonnes would be exhausted by ~2160.

One way in which this finite resource could be extended is by incorporating thorium as a nuclear fuel. Present estimates suggest that global thorium reserves total 6.4–7.5 million tonnes; however, due to its long half-life, it is expected that thorium is 3–4 times more abundant in the Earth's crust than uranium. Thorium is traditionally associated with closed nuclear fuel cycles, where fissile isotopes (such as ^{233}U formed from ^{232}Th, and ^{239}Pu and potentially other minor actinides primarily formed from ^{238}U) are recovered from the SNF and reused. Advocates claim that Th-based fuels offer advantages over U-based fuels. Foremost, since ^{232}Th has a larger thermal neutron capture cross-section than ^{238}U, ^{233}U can be bred more efficiently from ^{232}Th within thermal spectra than ^{239}Pu can be bred from ^{238}U. Given that ^{233}U is formed, it is often mentioned that less plutonium and fewer minor actinides are formed and these elements form the bulk of long-lived radiotoxicity, spontaneous neutron emission and decay heat (over 1000–100,000 years) of SNF, see e.g. Kamei and Hakami (2011). In terms of economics, thorium is currently characterised as a waste by-product, typically from rare-earth element processing, and it is suggested that the introduction of thorium has the potential to suppress the volatility of uranium prices. Thorium has been commonly ascribed as having enhanced proliferation resistance due to the facts that: (1) less LEU fuel is contained within the reactor, yielding smaller amounts of plutonium; (2) the ^{233}U that is bred within the fuel is denatured with unreacted ^{238}U; and (3) the short-lived isotope ^{232}U is also formed, the daughter products of which (particularly ^{208}Tl) add an additional radiological barrier.

For countries that want to adopt new nuclear energy systems, open nuclear fuel cycles are typically considered due to their lower infrastructure requirements and the significantly greater costs of reprocessing and refabrication than those of direct disposal. Therefore, the question arises as to whether thorium can be utilised in an open nuclear fuel cycle and incorporated in existing or novel nuclear energy technologies. It should be noted that this work treats the open nuclear fuel cycle in its strongest sense, i.e. plutonium disposition fuel cycles are considered to be out of scope, due to the need for prior SNF reprocessing. From a recent review paper (Ashley et al., 2013), a number of technology families have been highlighted that could prospectively use open Th–U-based fuel cycles. These include: (1) existing light water reactors (LWRs), (2) novel heavy-water-moderated, light-water-cooled reactors, and (3) novel high-temperature gas-cooled reactors.

This paper seeks to compare three candidate technologies operating with open Th–U-based nuclear fuel cycles to a 'reference' U-fuelled nuclear energy system over various performance indicators. The Th–U-fuelled technologies include AREVA's European Pressurised Reactor (EPR), the Indian Advanced Heavy Water Reactor (AHWR), and General Atomics' Gas-Turbine Modular Helium Reactor (GT-MHR). The reference U-fuelled system chosen was an EPR. Section 2 provides an overview of the fuel cycle modelling software, ORION, that was used in this work to derive mass flows and separative work units, isotopics associated with the SNF, and uranium and plutonium vectors for assessing the proliferation resistance of the SNF. Section 3 outlines the reactor systems further, the simulation techniques used and the parameters adopted in the neutronic analyses. Section 4 covers the mass flows of uranium, thorium, and separative work units for each of the four nuclear fuel cycles that are reported. Section 5 covers the isotopics of the SNF and the corresponding volumes, radiotoxicities, spontaneous neutron emission rates, and decay heats, and the potential issues surrounding deep geological disposal. Section 6 outlines an economic analysis of the fuel cycles and the corresponding nuclear energy systems to yield levelised nuclear fuel cycle costs and levelised costs of electricity. Section 7 covers the proliferation resistance methodology that was developed at the UK National Nuclear Laboratory (NNL) and is applied to each of the four nuclear fuel cycles. Finally, Section 8 provides a discussion of the results of Sections 4–7 and indicates the areas where open Th–U-based nuclear fuel cycles will need to be more competitive if they are to compete with open U-based cycles.

2. Fuel cycle simulation with ORION

ORION is a fuel cycle modelling code developed at NNL. The code performs inventory analysis to determine the throughput of material throughout a number of facilities in the nuclear fuel cycle, including storage buffers (that can represent the mine, mill and deep geological repositories), fuel fabrication facilities, reactors, and reprocessing facilities. For modelling the isotopic inventories within a reactor, ORION requires burn-up-dependent, shielded cross-sections produced by post-processing the results from deterministic or Monte-Carlo-based neutronic analyses of the reactor core. ORION has the capability to calculate the radiotoxicity, toxic potential, activity, spontaneous neutron emission rate and decay heat throughout the fuel cycle, as ~2500 isotopes including fission products and actinides are tracked. For radiotoxicity calculations, doses are evaluated using ingestion conversion coefficients provided in International Commission on Radiological Protection (1996). For decay heat and neutron emission rates, data from the JEF-2.2 Nuclear Data Library (OECD-NEA, 2000) are used.

A major strength of ORION is its ability to model complicated multi-reactor, multi-recycle options than can be used in energy pathway analyses, as outlined in Gregg and Grove (2012). This paper will outline its use in novel, open Th–U-based nuclear fuel cycles.

3. Selection of nuclear energy systems fuelled with thorium and LEU

Nuclear energy technologies that can potentially utilise open Th–U-based nuclear fuel cycles are described in Ashley et al. (2013) and references therein. Three different reactor technologies that broadly cover LWRs, heavy-water-moderated, light-water-cooled reactors, and high-temperature gas-cooled reactors have been selected for this study, these are respectively: AREVA's EPR, the Indian AHWR, and General Atomics' GT-MHR. In each case, the maximal enrichment of the uranium component of the fuel is ~20% ^{235}U.[2] As a reference for comparison, these three cases will be compared with a U-fuelled (with ^{235}U = 5%) EPR. In general, detailed simulations for these reactor configurations have previously been performed by a number of groups and these are highlighted in the following sub-sections. The neutronic simulations outlined in this work were performed to generate burn-up-dependent cross-sections required to determine the composition of the SNF and mass flows of feed materials.

3.1. Reference LEU-fuelled nuclear reactor: The EPR

The reference system considered in this study is AREVA's EPR, which is prospectively going to be constructed in the UK at Hinkley Point in Somerset and Sizewell in Suffolk. The parameters used to model this reactor are detailed in Table 1, the majority of these being taken from the submission to the UK Generic Design Assess-

[2] In this paper, all compositions with the exception of those in Table 5 are quoted in wt%.

Table 1
Parameters used in modelling the reference AREVA EPR.

Reactor parameters	
Thermal power	4500 MW(th)
Electrical power	1630 MW(e)
Load factor	90%
Number of assemblies	241
^{235}U content (equilibrium)	5.0%
^{235}U content (start-up)	2.1%, 3.2%, 4.2%, 5.0%
Core mass	127.15 t_{HM}
Refuelling scheme	3-batch over 4.5 years
Number of assemblies with 8% Gd_2O_3	144
UO_2 density	10.2 g/cm^3
Power density	35.4 W/g_{HM}
Active core length	4.2 m
Coolant and moderator	Light water
Average discharge burn-up	51.5 GWd/t_{HM}
Operating temperature for fuel	626.9 °C
Operating temperature for coolant	313.7 °C
Assembly parameters (all dimensions reported are at 20 °C)	
Number of pins	265
Assembly layout	17 × 17
Fuel rod diameter	9.50 mm
Fuel pellet diameter	8.19 mm
Diametral gap	0.17 mm
Cladding thickness	0.57 mm
Pin pitch	12.6 mm
Assembly pitch	215 mm
Cladding material	Zircaloy M5

ment (AREVA, 2007) with gaps being filled from the earlier design in Sengler et al. (1999). Neutronic simulations of this system were performed using WIMS 9 (Newton and Hutton, 2002), with nuclear data from the JEF-2.2 library (OECD-NEA, 2000). Results from these simulations were cross-checked with a separate set of calculations using CASMO-4 (Rhodes and Edenius, 2003) with nuclear data also from the JEF-2.2 library, as used in Gregg and Grove (2012).

During equilibrium operation, fresh nuclear fuel containing ^{235}U = 5.0% is loaded every 18 months on a three-batch scheme.[3] For the reactor start-up, the associated uranium enrichments of the initial core are ^{235}U = 2.1%, 3.2%, 4.2%, and 5.0% (AREVA, 2007). The initial enrichments used in the reactor start-up phase are accounted for when determining the mass flows of the feed material. However, only the isotopic composition of the SNF from the equilibrium phase of the reactor has been analysed. This means that the absolute radiotoxicity, neutron emission rates and decay heats would be very slightly overestimated (when averaged over the whole life of the reactor).

3.2. The EPR fuelled with LEU and thorium

The starting point for this comparison was a Th–U core design based on an optimised Westinghouse four-loop PWR designed to minimise waste and enhance proliferation resistance (Todosow and Kazimi, 2004). As the AREVA EPR was used as the reference technology in this study, the Westinghouse core design was upscaled and mapped to match that of the EPR core. The main parameters used in these simulations are listed in Table 2.

In the original 193-assembly Westinghouse core design, there were 84 seed assemblies (containing annular UO_2 fuel pellets enriched to 20% ^{235}U with axial reflector blankets of natural U) and 109 blanket assemblies (containing blended ThO_2/UO_2 fuel, in the ratio 87:13, with the uranium enrichment set to 10% ^{235}U). For the 241 assemblies within the EPR, this corresponds to 105 seed assemblies and 136 blanket assemblies. In both the Westinghouse

Table 2
Parameters used in modelling the AREVA EPR whole-assembly seed-blanket design, fuelled with LEU and thorium.

Reactor parameters	
Thermal power	4500 MW(th)
Electrical power	1630 MW(e)
Load factor	90%
Number of seed assemblies	105
Number of blanket assemblies	136
Seed ^{235}U enrichment	20%
Blanket ^{235}U enrichment	7.65%
Blanket UO_2/ThO_2 ratio	83:17
Seed mass	33.27 t_{HM}
Blanket mass	84.85 t_{HM}
Seed refuelling scheme	3-batch over 4.5 years
Blanket refuelling scheme	1-batch over 13.5 years
Seed fuel density	10.3 g/cm^3
Blanket fuel density	9.4 g/cm^3
Seed power density	87.91 W/g_{HM}
Blanket power density	18.56 W/g_{HM}
Active core length	4.2 m
Coolant and moderator	Light water
Seed discharge burn-up	140 GWd/t_{HM}
Blanket discharge burn-up	88 GWd/t_{HM}
Operating temperature for fuel	626.9 °C
Operating temperature for coolant	313.7 °C
Assembly parameters (all dimensions reported are at 20 °C)	
Number of pins	265
Assembly layout	17 × 17
Seed fuel rod diameter	9.00 mm
Seed pellet radius (outer annulus)	3.85 mm
Seed pellet radius (inner annulus)	2.20 mm
Blanket fuel rod diameter	10.60 mm
Blanket pellet radius	4.65 mm
Interstitial gap	0.08 mm
Cladding thickness	0.57 mm
Pin pitch	12.6 mm
Assembly pitch	215 mm
Cladding material	Silicon carbide

and EPR design, 17 × 17 assemblies with identical cross-sngth of the Westinghouse assembly described in Todosow and Kazimi (2004) is 3.81 m compared to the active length of 4.2 m in the EPR assembly.[4]

In a similar manner to the up-scaling of the number of assemblies, the fractional lengths of the poisoned, unpoisoned, and reflective regions (shown in Fig. 1) remain the same. The burnable poison used in these assemblies is Er_2O_3. Similarly, the same refuelling scheme is assumed for the EPR. Due to the high discharge burn-ups of the seed and blanket assemblies, silicon carbide has been assumed as the cladding material. Although silicon-carbide-based cladding requires significant research and development, such materials may become viable in the next 10–20 years. Further details on the development status of silicon-carbide-based cladding materials can be found in Hallstadius et al. (2012).

For the neutronic simulation of this core, the deterministic code WIMS 9 (Newton and Hutton, 2002) was used with cross-sections from the JEF-2.2 library (OECD-NEA, 2000). Cross-sections were generated using a supercell corresponding to an infinite 'chequerboard' of seed and blanket assemblies (as shown in Fig. 2), such that interface effects between assemblies were explicitly modelled in WIMS. The subgroup method was used for 172-group cross-section preparation for treatment of heterogeneous geometry resonance interaction effects between ^{232}Th, ^{233}U, ^{235}U and ^{238}U (Powney and Newton, 2004). As the assemblies were treated only in two dimensions, the axial blanket region and poisoned region of

[3] In Ref. (Sengler et al., 1999) a four-batch fuelling scheme is posited. We believe the discharge burn-ups for this scheme would be too large (~70 GWd/t_{HM}) compared to the present maximal discharge burn-up of 65 GWd/t_{HM}.

[4] In Table B2.1.4 of (Todosow and Kazimi, 2004) the active length of the fuel pin is quoted as 365.76 cm, which differs from the lengths provided in Fig. B2.1.9 of the same work which total 381 cm.

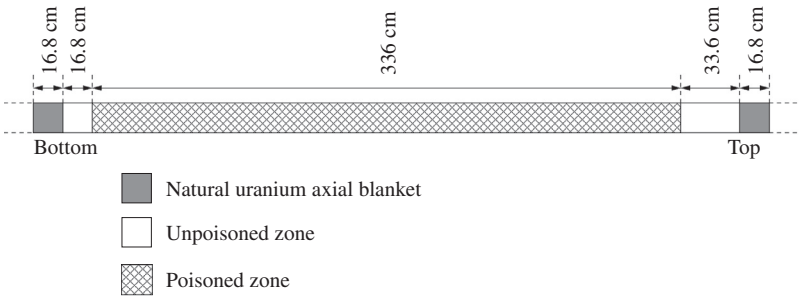

Fig. 1. Schematic diagram of the seed fuel pin axial zoning for the AREVA EPR whole-assembly seed-blanket design, fuelled with LEU and thorium.

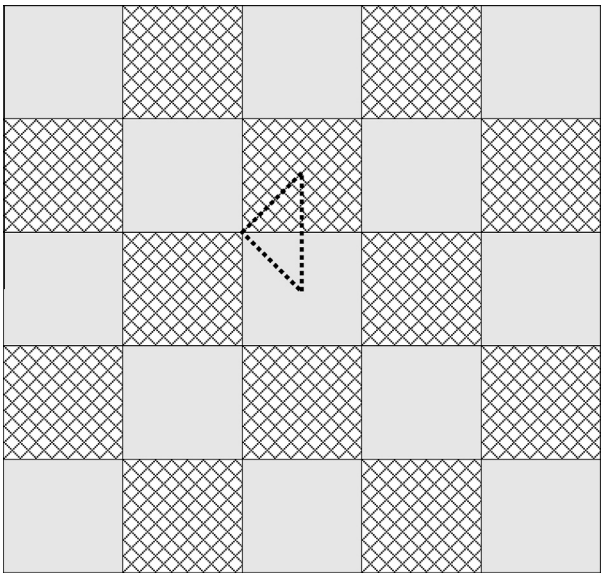

Fig. 2. Schematic diagram of the infinite chequerboard whole-assembly seed-blanket design (with translational boundary conditions) used in the neutronic calculations of the EPR with UO_2 and ThO_2. The dashed line shows the smallest unit cell (with reflective boundary conditions).

the seed assembly were "smeared" into a homogeneous region, which is appropriate for fuel cycle calculations.

On initial simulations of the blanket assembly, it was observed that the ^{233}U content exceeded the 12% limit for LEU containing ^{233}U, as described further in Section 7 and Ashley et al. (2012). Therefore, the ratio of thorium to uranium was changed from 87:13 to 83:17, with the ^{235}U enrichment decreased from 10% to 7.65% to match the fissile fraction and to denature the uranium component. We note that the discharge burn-up of the blanket may be slightly affected by this change.

For standard commercial reactors, especially typical PWRs, codes exist for performing full-core analyses to determine the optimal loading patterns and exact discharge burn-ups. However, the nested Th–U fuel assembly design is novel and the highly heterogeneous nature of the core, with large differences in occupancy times of the seed and blanket assemblies, make full-core calculations non-trivial. Determining an optimal in-core fuel management scheme and corresponding discharge burn-ups was beyond the scope of this work. We therefore assume the same discharge burn-ups as that of the Westinghouse design, i.e. a discharge burn-up of 140 GWd/t_{HM} for the seed assemblies and a discharge burn-up of 88 GWd/t_{HM} for the blanket assemblies. We note that this particular design is not optimised and that further full-core calculations are required to determine accurately the exact discharge burn-ups of seed and blanket assemblies. For completeness, the thermal–hydraulic feasibility of the up-scaled design should also be evaluated.

3.3. India's AHWR fuelled with LEU and thorium

The parameters used to model the AHWR are listed in Table 3. These parameters are taken from Bhabha Atomic Research Centre (2012), International Atomic Energy Agency (2012b), Thakur et al. (2011). Due to the relatively large central displacer rod, as shown in Fig. 3, the lattice code available was not able to model this particular geometry. Therefore, the Monte Carlo computer code MCNPX version 2.7.0 (Pelowitz, 2007; Pelowitz et al., 2011) was used instead. Nuclear data for these calculations were taken from the JEF-2.2 library (OECD-NEA, 2000). Further details on this model can be found in Cowper (2012).

Table 3
Parameters used in modelling the AHWR fuelled with LEU and thorium.

Reactor parameters	
Thermal power	920 MW(th)
Electrical power	300 MW(e)
Load factor	90%
Number of fuel clusters	444
^{235}U enrichment	19.75%
Start-up UO_2/ThO_2 ratio	13:87
Equilibrium UO_2/ThO_2 ratio	21.8:78.2
Core mass	51.77 t_{HM}
Refuelling scheme	10-batch over 10 years
Fuel density	9.4 g/cm^3
Power density	17.77 W/g_{HM}
Active core length	3.5 m
Moderator	Heavy water
Coolant	Light water
Discharge burn-up	64 GWd/t_{HM}
Operating temperature for fuel	450 °C
Operating temperature for coolant	285 °C
Coolant density	0.45 g/cm^3
Moderator temperature	67.5 °C
Moderator density	1.089 g/cm^3
Assembly parameters (all dimensions reported are at 20 °C)	
Cluster pin arrangement	12 (inner) 18 (middle) 24 (outer)
Number of pins with 5% Gd content	2 (inner)
Fuel rod diameter	11.20 mm
Pellet radius	4.90 mm
Interstitial gap	0.10 mm
Cladding thickness	0.60 mm
Cluster pin-pitch circle diameter	51.4 mm (inner) 77.4 mm (middle) 103.7 mm (outer)
Zircaloy centre (outer radius)	9.00 mm
Zircaloy tube (outer radius)	18.00 mm
Cladding material	Zircaloy-2
UO_2/ThO_2 ratio	30:70 (inner) 24:76 (middle) 16:84 (outer)

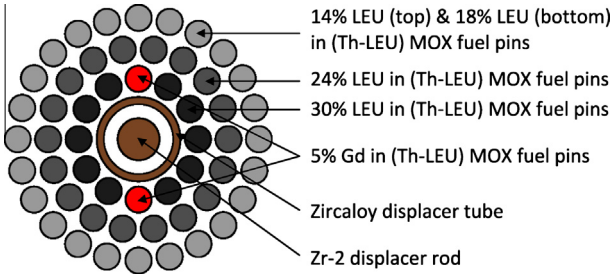

Fig. 3. Schematic diagram of the AHWR cluster. The LEU to thorium ratio is: 30:70 for inner fuel pins (shown as black circles), 24:76 for middle fuel pins (shown as dark grey circles), and 16:84 for outer fuel pins (shown as light grey circles). Solid red circles denote fuel pins that contain 5 wt% Gd_2O_3. (For interpretation of the references to colour in this figure legend, the reader is referred to the web version of this article.)

In normal operation, the AHWR is expected to operate with on-line refuelling, with an expected average discharge burn-up of 64 GWd/t_{HM} and an estimated 46 of the 444 bundles discharged every year. To account for this within ORION, a comparable off-line refuelling scheme (with an appropriate load factor) is adopted, and we approximate this to a scheme in which one tenth of the core is refuelled every year. This simplification will only affect spent fuel compositions during the initial and final years of operation whilst the reactor is not at equilibrium.

During start-up operation, two types of fuel are used. Both consist of 13.0% LEU (enriched to 19.75% ^{235}U) and 87.0% thorium, with differing amounts of burnable poison (Gd_2O_3). These are subsequently replaced with equilibrium clusters with 21.8% LEU and 78.2% thorium (as detailed in Table 3). In a similar fashion to the reference EPR described in Section 3.2, the start-up composition is considered within the material flow of the fuel cycle but the composition of the waste form considered will only be from the equilibrium fuel form.

3.4. The General Atomics' GT-MHR fuelled with LEU and thorium

The parameters used in the simulation of the GT-MHR are presented in Table 4, with the material properties of the TRISO fuel and fuel blocks listed in Table 5. The geometry of the core design used is the exact model reported in Talamo and Gudowski (2005). In terms of the neutronic simulations, MCNPX version 2.7.0 (Pelowitz, 2007; Pelowitz et al., 2011) was used, which differs from the use of MCNP4c3 (Breismeister, 2000) and MCB1C (Cetnar et al., 1999) used in Talamo and Gudowski (2005). For both simulations, the JEF-2.2 library was used (OECD-NEA, 2000).

The equilibrium fuel cycle is based on a three-batch cycle lasting a total of 2.75 years, which is shown diagrammatically in Fig. 4. As indicated, ~4.08 tonnes of SNF is discharged per batch, with ~2.04 tonnes consisting of once-through "driver fuel" (DF) and ~2.04 tonnes of twice-through "post-driver fuel" (PDF). It should be noted that the route to achieving the equilibrium fuel cycle, presented within Figs. 6 and 7 of Talamo and Gudowski (2005), is somewhat complicated. In summary, ~30 tonnes of DF is discharged over the first eight years and this is accounted for within the mass flow analysis. Within the waste-form analysis, only the equilibrium DF and PDF are considered.

4. Mass flows

In addition to the enrichments, core masses, and refuelling schemes presented in Tables 1–4, the parameters listed in Table 6 were used to determine the mass flow of uranium and separative work required over the whole lifetime of the reactor and for each kWh(e) generated.

Table 4
Parameters used in modelling the GT-MHR fuelled with LEU and thorium.

Reactor parameters	
Thermal power	600 MW(th)
Electrical power	286 MW(e)
Load factor	90%
Number of fuel blocks	108
^{235}U enrichment	20%
UO_2/ThO_2 ratio	60:40
Core mass	18.40 t_{HM}
Refuelling scheme (equilibrium)	Three-batch over 330 days. Half of the spent fuel is irradiated for a further three batches (see Fig. 4).
Fuel density	10.2 g/cm^3
Power density	32.6 W/g_{HM}
Core active height	7.93 m
Fuel block parameters (all dimensions reported are at 20 °C)	
Hexagonal fuel blocks	
Number of fuel blocks	36 (inner) 36 (middle) 36 (outer)
Width	0.36 m
Height	7.93 m
Interstitial gap	1.0 mm
Fuel blocks	
DF pins (with/without control rod)	128/144
PDF pins (with/without control rod)	64/72
Coolant channels (with/without control rod)	95/108
Pins	
Radius	6.22 mm
Height	7.93 m
Distance between pins	32.56 mm
Hole radius (fuel/coolant channel)	6.35 mm/7.95 mm
TRISO particles	
Kernel radius (fuel/control rods)	0.15 mm/0.30 mm
Width porous carbon layer (fuel/control rods)	0.064 mm/0.050 mm
Width inner pyrocarbon layer (fuel/control rods)	0.026 mm/0.015 mm
Width ZrC layer	0.031 mm
Width outer pyrocarbon layer	0.055 mm
Distance between particles (fuel/control rods)	1.34 mm/1.20 mm
Packing fraction (fuel/control rods)	37.55%/23.57%
Control rods	
Start-up (inner ring)	12
Operational (outer moderator reflector ring)	36
Shutdown (central ring/outer ring)	6/12
Internal radius (start-up/operational/shutdown)	0 mm/26.4 mm/0 mm
External radius	41.3 mm
Hole radius	50.5 mm
Distance from the centre of the hexagon	97.56 mm
Height at beginning of life (start-up/operational/shutdown)	0 mm/0 mm/0 mm

The losses within conversion, enrichment and fuel fabrication are taken from OECD-NEA (1994). For the losses in conversion, 0.5% is expected to be an upper limit (Shropshire et al., 2009). Typical values for the ^{235}U content of the tails are in the range 0.25–0.30%. In this work, the lower value of 0.25%, used in the long-term demand scenarios of the World Nuclear Association (World Nuclear Association, 2009), is adopted. The separative work for the enrichment process required for these fuel cycles, as derived in Benedict et al. (1981), is:

$$\Delta V = M_P V_P + M_T V_T - M_F V_F \quad (1)$$

where M_P, M_T, and M_F refer to the masses and V_P, V_T, and V_F refer to the "value functions" of the product, tails and feed materials,

Table 5
Properties of materials that comprise the LEU (60%) and thorium (40%) fuelled GT-MHR.

Material	Atomic percentage (%)	Initial density (g/cm^3)
TRISO kernel	^{235}U (4.2857); ^{238}U (17.143) ^{232}Th (14.286); ^{16}O (64.286)	10.2
TRISO porous graphite	C (100)	1
TRISO pyrocarbon	C (100)	1.85
TRISO ZrC	Zr (50); C (50)	6.56
Graphite	C (100)	1.74
Control rods	^{10}B (71); ^{11}B (8); ^{12}C (20)	2.47

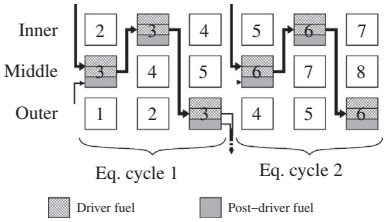

Fig. 4. Equilibrium fuel cycle for the GT-MHR. Fresh fuel is loaded in the middle ring in batch 1, shuffled to the inner section for batch 2, and shuffled to the outer section in batch 3, before being discharged or re-used as PDF.

respectively. The value function for each of these components, V_X, is:

$$V_X = (1 - 2w_X)\ln\left(\frac{1 - w_X}{w_X}\right) \quad (2)$$

where w_X is the relative weight of each component.

The EPR and GT-MHR are listed as having lifetimes of 60 years (AREVA, 2012; General Atomics, 2002) and the AHWR 100 years (International Atomic Energy Agency, 2012b). Therefore, to allow as fair a comparison as possible, and due to the blanket component of the EPR fuelled with UO_2/ThO_2 lasting for 13.5 years, for all fuel cycles in this study, the reactor lifetimes were centred as close to 67.5 years as possible (i.e. 67.5 years for the EPR fuel cycles, 67 years for the AHWR, and 66.7 years for the GT-MHR). This should yield a fair comparison as each of the fuel cycles are complete and in equilibrium, and the results are normalised to each kWh generated (noting that the economics analysis in Section 6 accounts for discounting). For all technologies considered in this work, the lifetimes are significant increases on those of current technologies; therefore it remains to be seen whether such lifetimes are achievable. The amounts of uranium, thorium, and separative work required for each nuclear fuel cycle in this study are presented in Fig. 5, with the corresponding amounts of uranium, thorium, and separative work capacity to generate 1kWh(e) being shown in Fig. 6.

From Fig. 6 it is evident that the Th–U-fuelled AHWR requires the least amount of uranium ore per kWh(e) generated. To highlight the sensitivity of this metric, if the core occupancy of the U-fuelled EPR were to be extended from 4.5 to 5 years (with the average discharge burn-up increasing from 51.5 GWd/t$_{HM}$ to 58.7 GWd/t$_{HM}$, and assuming the same initial enrichments and load factor) then the U-fuelled EPR would require less uranium ore per kWh(e). Due to the requirement of uranium enriched to ~20% ^{235}U for the Th–U-fuelled systems, the U-fuelled reference EPR requires the smallest amount of separative work units per kWh(e) generated.

In the case of the AHWR, the ratio of the average discharge burn-up (64 GWd/t$_{HM}$) to the fissile fraction of the fuel initially loaded (4.3%) is greater than that seen for the reference EPR in this study (51.5 GWd/t$_{HM}$ for 5% ^{235}U). The requirement of ^{235}U enriched to 19.75% yields a greater amount of separative work per kWh than for the reference EPR. An open question is how a

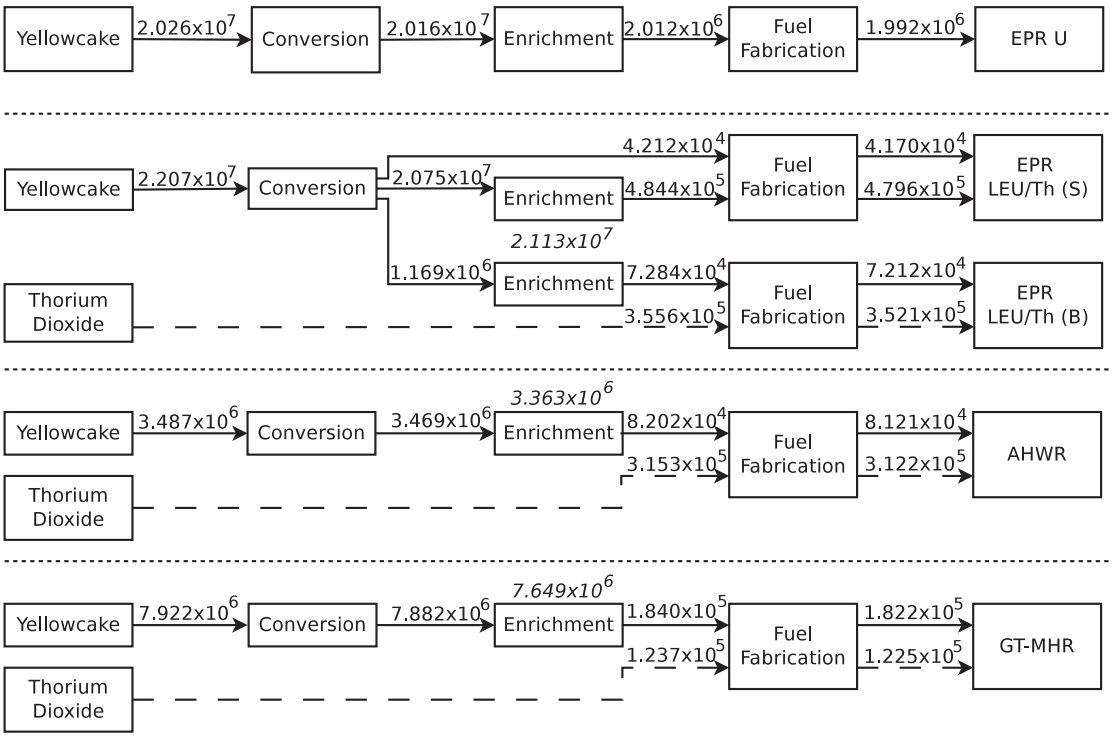

Fig. 5. Mass flows and separative work over the whole lifetime for the four reactor systems. Normal text denotes either the mass of uranium (in kgU) or the mass of thorium (in kgTh). Italicised text denotes the separative work units required (in kgSWU). To convert these numbers into correct material form: 1 kgU = 1.1344 kgUO_2; 1 kgU = 1.1792 kgU_3O_8; 1 kgU = 1.4789 kgUF_6; 1 kgTh = 1.1379 kgThO_2.

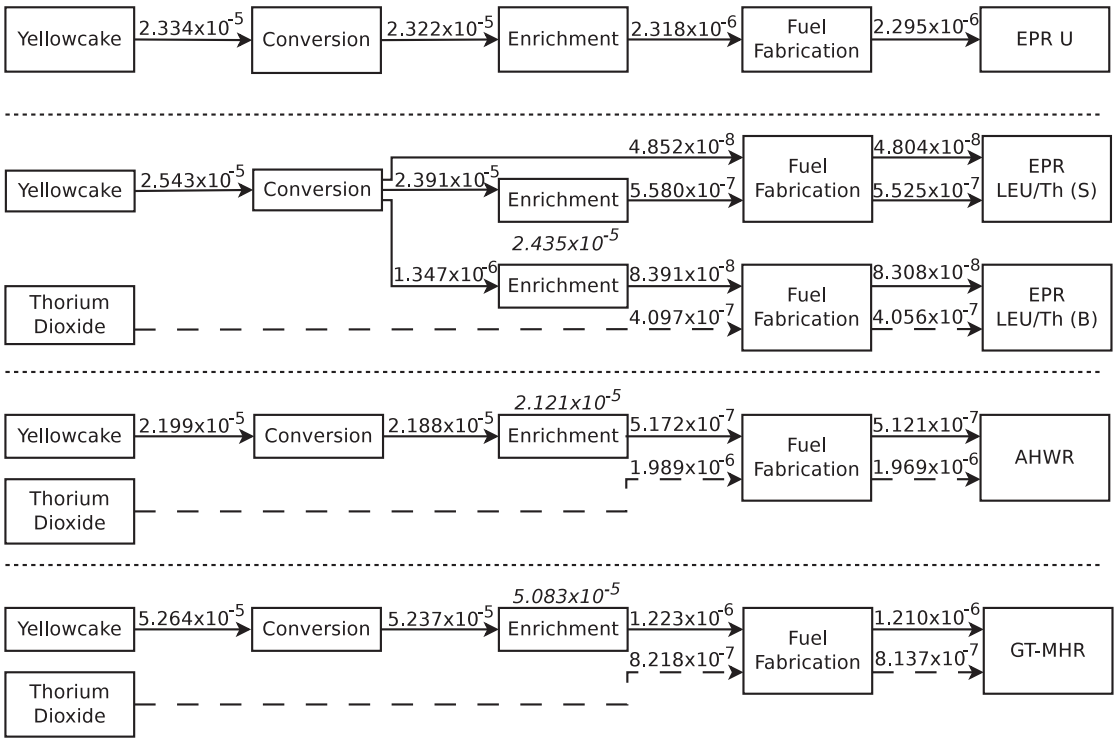

Fig. 6. Mass flows and separative work to generate 1 kWh(e) for the four reactor systems. Normal text denotes either the mass of uranium (in kgU) or the mass of thorium (in kgTh). Italicised text denotes the separative work units required in kgSWU.

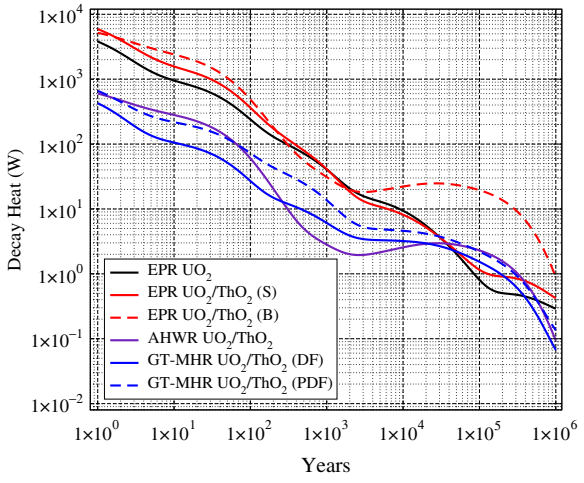

Fig. 7. Decay heats per assembly discharged for the four nuclear energy systems studied in this work. (S) denotes the seed assemblies and (B) denotes the blanket assemblies of the Th–U-fuelled EPR. (DF) denotes the once-irradiated "driver" fuel and (PDF) denotes the "post-driver fuel" in the Th–U-fuelled GT-MHR. (For interpretation to colours in this figure, the reader is referred to the web version of this paper.)

Th–U-fuelled AHWR would compare to an equivalent U-fuelled AHWR, noting that fuel-cycle schemes for a U-fuelled AHWR are yet to be published.

It is particularly striking that the Th–U-fuelled GT-MHR requires significantly more uranium per kWh. This is due to the very low average discharge burn-up (~45 GWd/t_{HM}) compared to the initial fissile fraction of the loaded fuel (12%) for this configuration. Further work in determining the optimal balance between uranium, thorium and the discharge burn-up of the fuel in such systems is required.

Table 6
Parameters used in the analyses of mass flow of uranium and separative work required. Losses are taken from OECD-NEA (1994).

Parameter	Value
Loss in conversion	0.5%
Loss in enrichment	0.0%
Loss in fuel fabrication	1.0%
^{235}U content in tailings	0.25%
Lifetime of the EPR with UO_2	67.5 years
Lifetime of the EPR with UO_2/ThO_2	67.5 years
Lifetime of the AHWR with UO_2/ThO_2	67.0 years
Lifetime of the GT-MHR with UO_2/ThO_2	66.7 years
Load factor for all nuclear energy systems	90%
Construction time for all reactors	5 years
Lifetime electricity generated by EPR with UO_2	868.0 TWh
Lifetime electricity generated by EPR with UO_2/ThO_2	868.0 TWh
Lifetime electricity generated by AHWR with UO_2/ThO_2	158.6 TWh
Lifetime electricity generated by GT-MHR with UO_2/ThO_2	150.5 TWh

Finally, the EPR design with thorium and uranium was optimised such that the discharge burn-up was maximised with a view to minimising the amount of SNF. Thus, a Th–U-based core design where equivalent discharge burn-ups to that of the reference EPR are obtained could provide a fairer comparison. This is especially true if the required enrichment is well below 20%.

It should be stressed that this study is not exhaustive and there may be nuclear energy systems with different fuelling arrangements that could utilise thorium more successfully. One possible emerging technology where thorium could be considered in an open nuclear fuel cycle is the reduced-moderation boiling water reactor, where initial fuel cycle studies have shown promise (Lindley et al., 2013). However, a significant amount of research and development is needed, with a robust appraisal of the technical barriers that need to be overcome, before such technologies could be considered licensable. It should also be stressed that there is a significant gulf between that which is licensable and that which is viable.

5. Waste forms

The waste-form analysis covers four separate aspects of the SNF: decay heats, neutron emission rates, radiotoxicities, and volume. Sections 5.1–5.3 report the properties of the decay heats, spontaneous neutron emission rates and radiotoxicities for an individually discharged fuel assembly. Section 5.4 discusses, in absolute terms, the total volume of all assemblies discharged over the life of the reactor. Section 5.5 reports these four aspects in terms of normalised electrical output. It should be stressed that in the absence of a complete repository design and licensed package for each system being studied the following assessment should be seen as indicative rather than normative.

5.1. Decay heats per discharged assembly

The decay heat, as a function of time, of a single assembly discharged from each of the nuclear energy systems is shown in Fig. 7. It is evident that the decay heat of a single discharged assembly from the U-fuelled EPR is lower than that of a single discharged seed assembly and single discharged blanket assembly from the Th–U-fuelled EPR. For the Th–U-based blanket of the Th–U-fuelled EPR [UO_2/ThO_2 (B)], it is evident that for ~120 years the decay heats are higher than those from the seed [UO_2/ThO_2 (S)]. In this time period, although less SNF is discharged from the Th–U-fuelled EPR, the decay heats may either affect the amount of SNF which can be housed within a waste-form package (see Section 5.4) or would require the fuel to be kept in wet- or dry-storage for a longer period of time. This is explained by comparing the contribution of each individual isotope to the total decay heat for a seed assembly and a blanket assembly (as in Fig. 8), which shows that daughter products from ^{232}U, e.g. ^{216}Po, contribute ~10% of the decay heat in the blanket assembly at year 50. For all Th–U-based fuels, an increase in decay heat after 2000 years due to the ^{233}U decay chain could potentially have a detrimental effect on the performance of the backfill. For the AHWR and GT-MHR, the lower decay heats may allow for greater packing fractions in the waste form, as discussed further in Section 5.4.

5.2. Spontaneous neutron emission rates per discharged assembly

The spontaneous neutron emission rates, as a function of time, of a single assembly discharged from each of the nuclear energy systems are shown in Fig. 9. Neutron sources consist mainly of actinide nuclei which can undergo spontaneous fission, as seen in comparing the seed and blanket assemblies of the Th–U-fuelled EPR (shown in Fig. 10). Due to its longer irradiation time, the blanket contains greater amounts of minor actinides; ^{244}Cm is the dominant contributor for the first 150 years and thereafter ^{246}Cm up to ~40,000 years. In line with the decay heat observations in Section 5.1, the AHWR and GT-MHR have smaller spontaneous neutron emission rates than those seen in the EPR assemblies.

5.3. Radiotoxicities per discharged assembly

The radiotoxicity, as a function of time, of a single assembly discharged from each of the nuclear energy systems is shown in Fig. 11. Due predominantly to its lower discharge burn-up, the radiotoxicity of a single discharged assembly from the U-fuelled EPR is lower than that of a single discharged seed assembly and single discharged blanket assembly from the Th–U-fuelled EPR. After ~1000 years, contributions from the ^{233}U decay chain begin to dominate, as indicated by the ^{233}U contribution in Fig. 12. Similarly, the radiotoxicities of the AHWR and GT-MHR SNF are lower, mainly due to the smaller amounts of material discharged.

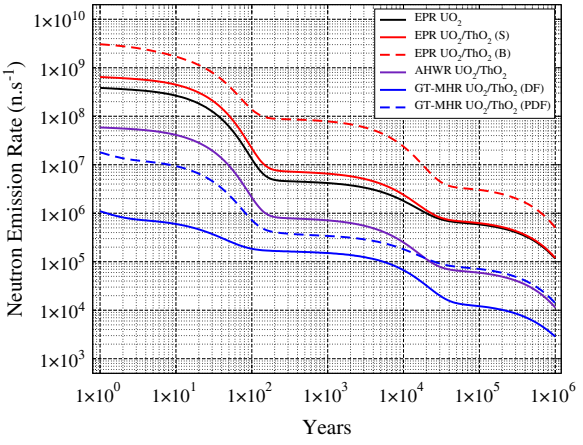

Fig. 9. Spontaneous neutron emission rates per assembly discharged for the four nuclear energy systems studied in this work. (S) denotes the seed assemblies and (B) denotes the blanket assemblies of the Th–U-fuelled EPR. (DF) denotes the once-irradiated "driver" fuel and (PDF) denotes the "post-driver fuel" in the Th–U-fuelled GT-MHR. (For interpretation to colours in this figure, the reader is referred to the web version of this paper.)

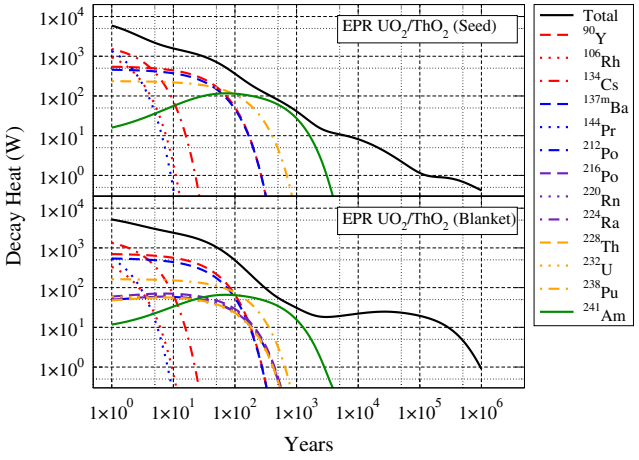

Fig. 8. Comparison of the isotopic contributions to the decay heats for the seed and blanket assemblies within the Th–U-fuelled EPR. (For interpretation to colours in this figure, the reader is referred to the web version of this paper.)

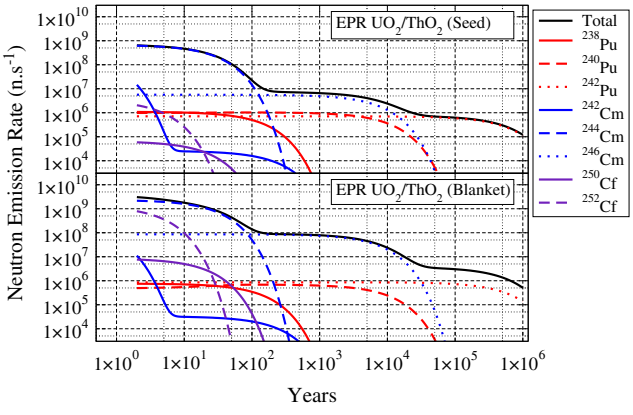

Fig. 10. Comparison of the isotopic contributions to the spontaneous neutron emission rates for the seed and blanket assemblies within the Th–U-fuelled EPR. (For interpretation to colours in this figure, the reader is referred to the web version of this paper.)

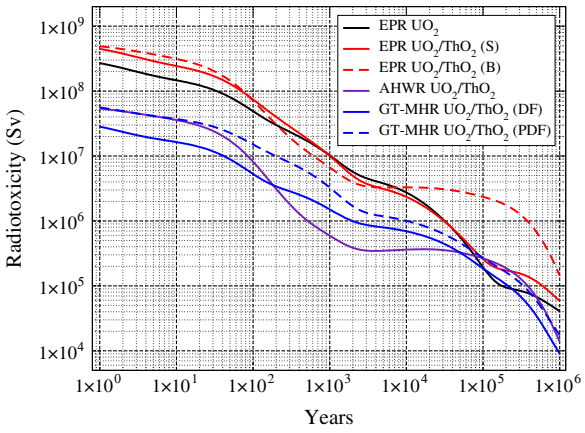

Fig. 11. Radiotoxicity of each assembly discharged for the four nuclear energy systems studied in this work. (S) denotes the seed assemblies and (B) denotes the blanket assemblies of the Th–U-fuelled EPR. (DF) denotes the once-irradiated "driver" fuel and (PDF) denotes the "post-driver fuel" in the Th–U-fuelled GT-MHR. (For interpretation to colours in this figure, the reader is referred to the web version of this paper.)

5.4. Volume of spent nuclear fuel

The parameters used in ascertaining the volumes of spent fuel for each nuclear system are presented in Table 7. In Table 8, data from the mass flows are used to determine the total volume of SNF discharged over the life of each reactor.

In accounting for the total numbers of SNF packages, various assumptions were needed to account for the dimensions of the waste-form package.

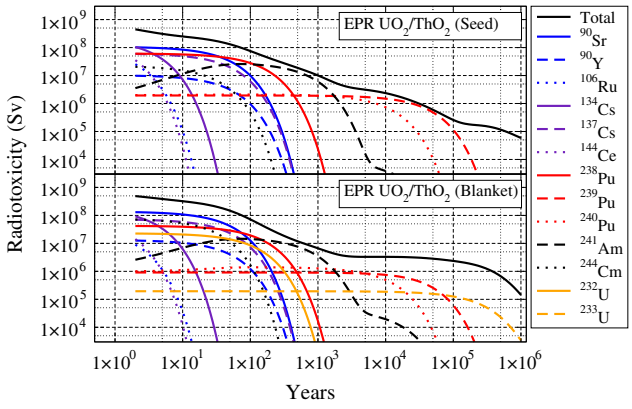

Fig. 12. Comparison of the isotopic contributions to the radiotoxicities for the seed and blanket assemblies within the Th–U-fuelled EPR. (For interpretation to colours in this figure, the reader is referred to the web version of this paper.)

Table 7
Dimensions of the nuclear fuel assemblies for the EPR, AHWR, and GT-MHR required for spent fuel analysis. AHWR cluster dimensions are taken from Sinha and Kakodkar (2006).

Reactor	Parameter	Value
EPR	Fuel assembly cross-sectional area	0.0458 m^2
	Fuel assembly length	4.80 m
AHWR	Cluster diameter	0.118 m
	Cluster cross-sectional area	0.0109 m^2
	Cluster length	4.30 m
GT-MHR	Fuel block diagonal length	0.416 m
	Fuel block cross-sectional area	0.112 m^2
	Fuel block length	7.93 m

Table 8
Expected numbers and volumes of nuclear fuel assemblies discharged over the lifetime of the four nuclear energy systems studied in this work. The italicised text shows the individual contributions of the seed assembles and blanket assemblies for the Th–U-fuelled EPR.

Nuclear energy system	Volume of single assembly (m^3)	Expected number of assemblies discharged	Total volume of assemblies discharged (m^3)
EPR with UO_2	0.2200	3761	8.27×10^2
EPR with UO_2/ThO_2 (total)	0.2200	2325	5.12×10^2
EPR with UO_2/ThO_2 (seed component only)	*0.2200*	*1645*	3.62×10^2
EPR with UO_2/ThO_2 (blanket component only)	*0.2200*	*680*	1.50×10^2
AHWR with UO_2/ThO_2	0.0470	3375	1.59×10^2
GT-MHR with UO_2/ThO_2	0.8900	2592	2.31×10^3

Two separate canisters for two different deep geological repositories were selected: the Svensk Kärnbränslehantering (SKB) KBS-3 (SKB, 2011) and Yucca Mountain (U.S. DOE, 2002). Details of the dimensions of the various waste-form packages are presented in Table 9. It is also assumed that the canisters can be filled completely, i.e. the fuel can be sufficiently cooled for a long enough period before encapsulation. If the fuel cannot be cooled for long enough, there will be limits on the allowable decay heat such that the inner bentonite surface temperature in the deep geological repository does not exceed 100 °C (temperature limit taken from Nuclear Decommissioning Authority (2009)).

For the EPR assemblies within the SKB design, slight modifications were needed to account for the comparatively longer fuel assembly than the generic PWR assembly length listed. This was done by adding the difference in canister length and assembly length of the generic PWR to the EPR assembly length. For the Yucca Mountain container, it is assumed that the 'long' container which houses 12 assemblies would suffice as is (given that it is designed to hold volumetrically larger Combustion Engineering and South Texas Project assemblies).

Table 9
Dimensions of the spent fuel canisters for both the SKB KBS-3 and Yucca Mountain repositories.

Waste-form package	Parameter	Value (m)
SKB PWR	Assembly length	4.443
SKB (2010)	Canister length	4.835
	Canister diameter	1.050
SKB EPR (assumed)	Assembly length	4.800
	Canister length	5.227
	Canister diameter	1.050
Yucca Mountain (long)	Assembly length	4.491–5.111
U.S. DOE (2002)	Canister length	5.651
	Canister diameter	1.330
Yucca Mountain EPR (assumed)	Assembly length	4.800
	Canister length	5.651
	Canister diameter	1.644
SKB AHWR (assumed)	Cluster length	4.300
	Canister length	4.692
	Canister diameter	1.050
Yucca Mountain AHWR (assumed)	Cluster length	4.300
	Canister length	4.840
	Canister diameter	1.318
Yucca Mountain GT-MHR	Fuel block total length	7.930
General Atomics (2002)	Fuel block element length	0.793
	Canister length	5.144
	Canister diameter	1.397

As the AHWR is traditionally associated with closed nuclear fuel cycles, no spent fuel packaging form has been suggested. The following is therefore an ansatz as to how such fuel may be arranged within a canister. As the AHWR has cylindrical assemblies, the optimal periodic packing fraction could be obtained by hexagonal packing. With this geometry, 7, 19, or 37 assemblies could be housed within one SKB canister. From Sections 5.1 and 5.2, the decay heat release rate and spontaneous neutron emission rate (both at 50 years) of an AHWR cluster are, respectively, roughly four and six times lower than those of an EPR assembly. Therefore, it is conceivable (as an upper estimate) that 19 assemblies could satisfactorily be housed in one canister. The only other adjustment required for the canister is a reduction in its height, as detailed above.

For the Yucca Mountain design, it has been assumed that 44 clusters could be housed within a single canister, i.e. the same canister geometry as for discharged assemblies from boiling water reactors.

For the GT-MHR, only the Yucca Mountain repository design is considered. It should be noted that, although the GT-MHR was treated as a continuous fuel block in Section 3.4, the fuel block is constructed of ten separate elements, held together by a support infrastructure. In General Atomics, (2002), it is suggested that 42 elements (4.2 fuel blocks) would be housed within a single canister design. The basis for choosing only this design is that even with an optimal packing fraction, the volume of waste is considerably greater than for EPR assemblies within the heavily self-shielded SKB canister.

The total volumes of packaged SNF from each nuclear energy system within this study (over their respective lifetimes) are presented in Table 10.

5.5. Comparison to normalised electrical output

The decay heats, neutron emission rates, radiotoxicities, and volume of SNF (presented in Sections 5.1–5.4 respectively) per kWh are presented in Fig. 13 and Table 10.

It is observed that there is a ~40% reduction in the volume of SNF for the Th–U-fuelled EPR compared to the reference U-fuelled EPR. As seen in Figs. 7 and 9, this is counter-balanced by the blanket assemblies having larger decay heat and spontaneous neutron emission rates, due to the significantly larger burn-up than in the reference EPR. However, the higher spontaneous neutron emission rate is counter-intuitive, given that Th-based fuels are normally expected to generate fewer minor actinides than equivalent U-based systems. The increase in the minor actinide contribution is attributed to the facts that the fuel is irradiated for significantly longer than conventional nuclear fuels and that the inner portion of the blanket assemblies appears more thermalised than the equivalent seed assemblies. In summary, although volumetrically less waste is generated, this advantage may be negated, as it may not be possible to use the same waste-form packaging as in the EPR reference scenario.

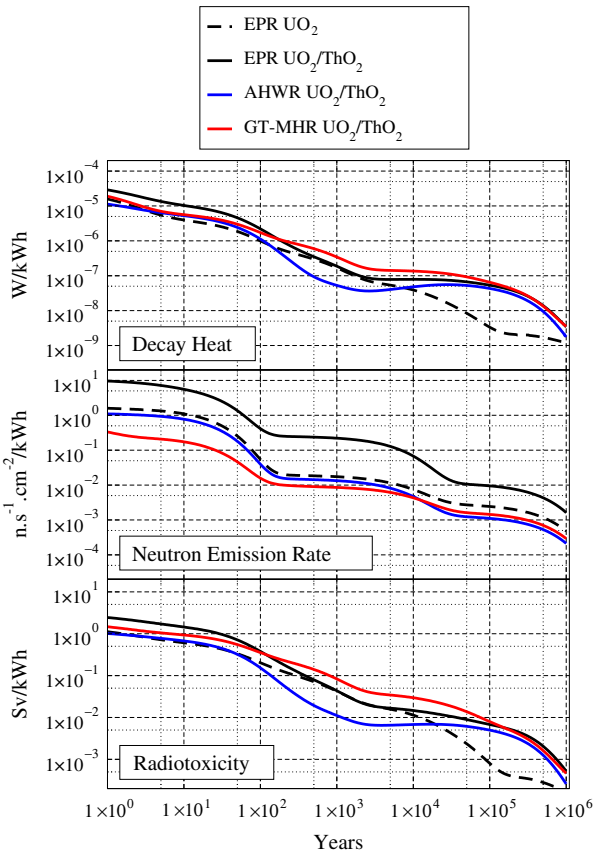

Fig. 13. Comparison of the decay heats, spontaneous neutron emission rates, and radiotoxicities (normalised to each kWh generated) for the four reactor systems considered in this work. (For interpretation to colours in this figure, the reader is referred to the web version of this paper.)

For the AHWR, studies involving the waste-form packaging have yet to be undertaken and so the analysis here is presented as a guide. A waste-form package containing 19 AHWR clusters would correspond to ~7% less SNF generated per kWh than for the reference U-fuelled EPR. A waste-form package containing 16 AHWR clusters (i.e. matching the total decay heat of the AHWR

Table 10
Characteristics of the waste-form packages and normalised packaged SNF associated with each nuclear energy system.

Nuclear energy system	Volume of package (m^3)	Assemblies per package	Total volume of packaged SNF (m^3)	Normalised volume of packaged SNF (m^3/kWh)
EPR with UO_2	4.53	4[a]	4.26×10^3	4.91×10^{-9}
	12.00	12[b]	3.76×10^3	4.33×10^{-9}
EPR with UO_2/ThO_2	4.53	4[a]	2.63×10^3	3.03×10^{-9}
	12.00	12[b]	2.33×10^3	2.68×10^{-9}
AHWR with UO_2/ThO_2	4.06	7[a]	1.96×10^3	1.23×10^{-8}
	4.06	19[a]	7.21×10^2	4.55×10^{-9}
	4.06	37[a]	3.70×10^2	2.34×10^{-9}
	6.60	44[b]	5.06×10^2	3.19×10^{-9}
GT-MHR with UO_2/ThO_2	7.88	4.2[b]	4.86×10^3	3.23×10^{-8}

[a] Waste-form package derived from the SKB canister design in Table 9.
[b] Waste-form package derived from the Yucca Mountain design in Table 9.

Table 11
Parameters used in modelling the LFCC in addition to the parameters listed in Table 6. The term kgiHM refers to "kilogram of initial heavy metal". Cost data is taken from nominal values provided in Shropshire et al. (2009). Lead times, lag times and losses are taken from OECD-NEA (1994). Discount rate is taken from De Roo and Parsons (2011a).

Parameter	Fuel cycle stage (i)	Units	Lower	Middle	Upper	Distribution
Cost of thorium dioxide	1	US$/kgTh	20	50	175	Triangular
Cost of yellowcake	1	US$/kgU	30	75	260	Triangular
Cost of conversion	2	US$/kgU	5	10	15	Uniform
Cost of enrichment	3	US$/kgSWU	85	110	135	Uniform
Cost of fuel fabrication (UO_2)	4	US$/kgU	200	250	300	Triangular
Cost of fuel fabrication (ThO_2/UO_2) for EPR Blanket and AHWR	4	US$/kgiHM	300	375	450	Triangular
Cost of fuel fabrication (ThO_2/UO_2) for GT-MHR[a]	4	US$/kgiHM	860	2870	2870	Triangular
Cost of transportation	5	US$/kgiHM	76	92	106	Triangular
Cost of interim storage of SNF	6	US$/kgiHM	150	300	500	Triangular
Cost of final disposition of SNF	7	US$/kgiHM	400	650	1000	Triangular
Lead time from mine/mill	1	years	2.0	2.0	2.0	Constant
Lead time in conversion	2	years	1.5	1.5	1.5	Constant
Lead time in enrichment	3	years	1.0	1.0	1.0	Constant
Lead time in fuel fabrication	4	years	0.5	0.5	0.5	Constant
Lag time in transportation	5	years	5.0	5.0	5.0	Constant
Lag time in interim storage of SNF	6	years	5.0	5.0	5.0	Constant
Lag time in final disposition of SNF	7	years	40	40	40	Constant
Losses in conversion	2	%	0.5	0.5	0.5	Constant
Losses in fuel fabrication	4	%	1.0	1.0	1.0	Constant
"Discount rate" (Weight-adjusted cost of capital)	1–7	%	7.6	7.6	7.6	Constant

[a] Value taken for a fabrication cost of 0.1 ¢ per kernel, as in Table D.1-3-1 in Shropshire et al. (2009).

waste-form package to the reference U-fuelled EPR waste-form package) would correspond to ~10% more SNF generated per kWh than the reference U-fuelled EPR. Therefore, it is fair to conclude that the volume of SNF per kWh discharged by the AHWR would be similar to that of the reference U-fuelled EPR.

Due to the considerably lower burn-up for the Th–U-fuelled GT-MHR, the amount of waste generated from this reactor is significantly greater than for the EPR and AHWR.

6. Economics

6.1. Estimation of the levelised fuel cycle costs

The methodology adopted for determining the levelised fuel cycle cost (LFCC) is based on that presented in OECD-NEA (1994). From this, the LFCC, C, can be determined using:

$$C = \frac{\sum_i \sum_t \frac{F_i(t)}{(1+r)^{t-t_0}}}{\sum_t \frac{E(t)}{(1+r)^{t-t_0}}} \quad (3)$$

where i is the stage of the fuel cycle, t denotes the year, t_0 denotes the commissioning year, F_i is the cost incurred in the ith stage of the fuel cycle, E is the electricity generated, and r is the discount rate (in this work, r is taken to be the weight-adjusted cost of capital). The cost incurred at each stage of the fuel cycle is given by:

$$F_i = x_i c_i l_i (1 + s_i)^{t-t_0} \quad (4)$$

where x denotes either the mass of feed, enriched product, or separative work units; c is the cost for each section of the fuel cycle; l denotes the loss of material at that stage; s is the escalation rate (i.e. the rate of increase in uranium price that is exogenous to discounting.); t denotes the date and t_0 is the baseline date. It is assumed that the baseline date is 01/01/2012, with the reactor starting operation on 01/01/2018. For front-end processes, t is defined as the date when fuel is loaded less the lead time; for back-end processes, t is defined as the date when the fuel is loaded, plus the residency time and lag time.

Each of the costs assumed here is listed in Table 11, where the currency is taken to be 2012 US$. As suggested in OECD-NEA (1994), only uranium has an escalation rate attributed, with a rate of 1.2% adopted. Note that it is assumed that the cost of enrichment per separative work unit for uranium enriched to ~20% ^{235}U is the same as that for uranium enriched to 5% ^{235}U. For blended ThO_2/UO_2 fuels, it is assumed that the cost of fabrication is 1.5 times that for normal UO_2 fuels, which is the upper limit provided in Shropshire et al. (2009), Lahoda (2004). For the annular UO_2 in the seed assemblies of the EPR, the fuel fabrication cost is assumed to be the same as for UO_2 fuel in the reference EPR.

Fig. 14 shows the comparison of the LFCC for each of the nuclear energy systems over the whole life of the reactor and normalised to each kWh generated. The normalised fuel cycle costs (assuming just the "middle" values quoted in Table 11) are 0.77¢/kWh for the U-fuelled EPR, 0.90¢/kWh for the Th–U-fuelled EPR, 0.99¢/kWh for the Th–U-fuelled AHWR, and 2.37¢/kWh for the Th–U-fuelled GT-MHR. From a Monte Carlo analysis using Simlab (EC JRC IPSC, 2011), the mean levelised costs (and uncertainties to one standard deviation) are: 0.97 ± 0.21 ¢/kWh for the U-fuelled EPR, 1.12 ± 0.25 ¢/kWh for the Th–U-fuelled EPR, 1.20 ± 0.22 ¢/kWh for the AHWR, and 2.61 ± 0.48 ¢/kWh for the GT-MHR.

For all Th–U-fuelled systems in this study, increases in LFCC are seen due to increased enrichment and greater fuel fabrication costs. The levelised cost of uranium ore is also slightly higher for the AHWR, due purely to discounting the longer fuel cycle length (i.e. a greater quantity of uranium is needed upfront than for the reference U-fuelled EPR). Due to increased uranium requirements for the Th–U-fuelled EPR and Th–U-fuelled GT-MHR in this study, any increase in the uranium price will cause further divergence in the LFCC for these systems.

Although the LFCC for Th–U-based fuels are higher, these values could be significantly underestimated. The assumed fuel fabrication cost for Th–U-based fuels is 1.5 times that of U-based fuels. This could also be significantly underestimated given: (1) the fact that fabrication of silicon-carbide cladding for the Th–U-fuelled EPR fuelled is currently not commercially viable (Hallstadius et al., 2012) and (2) the requirements of different U/Th ratios in the individual rings of the AHWR cluster (see Fig. 3).

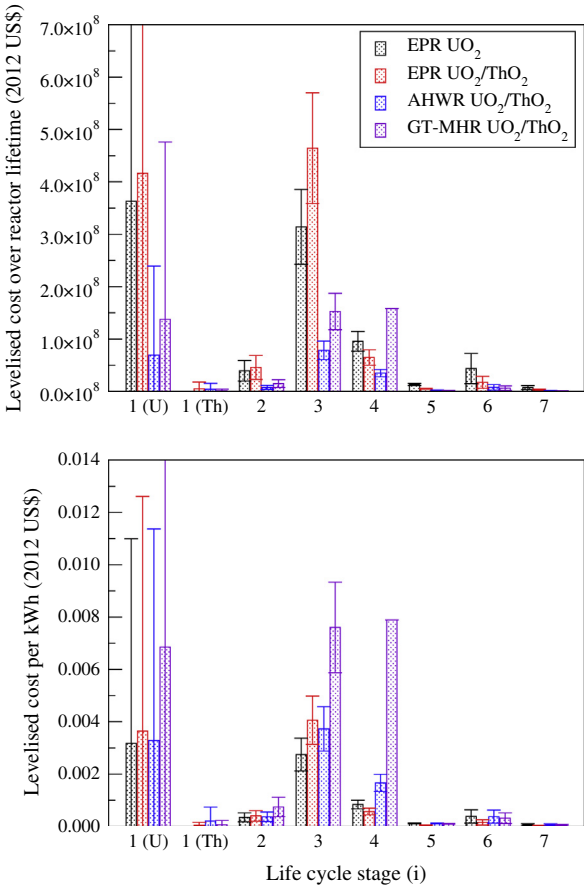

Fig. 14. Total levelised fuel cycle costs (top) and fuel cycle costs per kWh generated (bottom). The lifecycle stages correspond to those presented in Table 11. Error bars show the upper and lower limits of the values in Table 11. (For interpretation to colours in this figure, the reader is referred to the web version of this paper.)

6.2. From estimated levelised fuel cycle cost to estimated levelised cost of electricity

The levelised cost of electricity (LCOE) can be calculated using the formalism derived by De Roo and Parsons (2011a).[5] In particular, the LCOE is split into four levelised components: the reactor cost, fixed operation and maintenance (O&M) costs, variable O&M costs, and fuel cycle costs (as calculated in Section 6.1). The levelised cost components for the nuclear fuel cycles under consideration were calculated using the corresponding Excel spreadsheet (De Roo and Parsons, 2011b) with the parameters listed in Tables 6, 11, and 12. It should be noted that the decommissioning costs were included in the levelised net present value associated with reactor construction.

Using a similar procedure to the Monte Carlo analysis performed in Section 6.1, the mean LCOE (and uncertainty to one standard deviation) was found to be 121 ± 16 US$/MWh for the reference, U-fuelled EPR, 122 ± 17 US$/MWh for the Th–U-fuelled EPR, 137 ± 18 US$/MWh for the Th–U-fuelled AHWR, and 157 ± 14 US$/MWh for the Th–U-fuelled GT-MHR. The breakdown of the LCOE is presented in Table 13.

Estimating the LCOE is notoriously difficult given the limited information associated with the capital and operation costs for all of these reactor systems. Construction costs for nuclear energy systems in the West have significantly increased since the early 2000s, as detailed in Massachusetts Institute of Technology (2011), and there is a large geographical variation in construction costs (International Energy Agency, 2010) which could yield further inconsistencies. Due to the variation in the sources of information, as described in Table 12, the analysis presented should be considered as indicative (rather than definitive); with different assumptions the differences between the relative costs of the systems considered narrow or broaden.

[5] LCOE is commonly represented in units of US$/MWh, whereas LFCC is commonly represented in units of US¢/kWh. The conversion between these units is: 1US$/MWh = 0.1US¢/kWh

7. Proliferation resistance assessment

Proliferation resistance assessments of nuclear energy systems usually consist of qualitative assessments of quantitative data, and are by no means an exact science. In this work, the NNL proliferation resistance assessment methodology (Hesketh, 2012; Hesketh and Worrall, 2010; UK National Nuclear Laboratory, 2009) was used to assess the desirability of the plutonium and uranium components within the spent fuel for potential state proliferators. The methodology does not factor in the separative work capacity required for each system nor does it account for the amounts of dual-use materials as described in International Atomic Energy Agency (2012a).

The salient points of the NNL methodology are as follows. The NNL proliferation resistance score, $U(x)$, is defined as:

$$U(x) = -\log\left(V(x)A(x)\right) \tag{5}$$

where $V(x)$ is defined as the value function and $A(x)$ is defined as the access function. It should be noted that a higher value of $U(x)$ corresponds to a more proliferation resistant system.

The value function consists of the significant quantities (SQs) of specific nuclear materials discharged per GWy. From International Atomic Energy Agency (2002), one SQ is defined as: 8 kg for plutonium (which contains $\leqslant$80% ^{238}Pu) or ^{233}U; 25 kg for highly-enriched uranium (HEU) (^{235}U content >20%); 75 kg for LEU (^{235}U content $\leqslant$20%); 10,000 kg for natural U; and 20,000 kg for natural Th. Although other minor actinides (such as neptunium, americium and protactinium) can be considered as alternative nuclear materials, of which SQs can be attributed, such nuclei are not considered in this analysis.

From the fuel cycle modelling analysis using ORION, the quantities of uranium and plutonium per discharged amount of SNF for each nuclear fuel cycle, and their respective isotopic vectors, are presented in Tables 14 and 15. The corresponding SQs per GWy for each nuclear fuel cycle are presented in the first row of Table 16 for plutonium and Table 17 for uranium. It should be noted that the ^{232}U content is 884 ppm for the EPR blanket assemblies containing UO_2/ThO_2, 556 ppm for the AHWR with UO_2/ThO_2, 2 ppm for the GT-MHR UO_2/ThO_2 DF assemblies and 4 ppm for the PDF assemblies. The very low values for the GT-MHR can be explained by: (1) the increased amount of ^{235}U yielding a lower neutron fluence (a factor of ~3 less than for the AHWR, corresponding to ~1/9 the amount of ^{232}U), (2) a smaller fast neutron component of the spectrum (yielding an equilibrium ^{232}U cross-section 1/3 that of the AHWR), and (3) the low discharge burn-up for the driver fuel.

The access function is defined as follows:

$$A(x) = \frac{1}{\sqrt{10}}\exp([MT] + [TD] + [PC] + [PT] + [DP]) \tag{6}$$

where each of the terms listed in square brackets corresponds to accessibility barriers defined by the Proliferation Resistance and Physical Protection Evaluation Methodology Working Group of the Generation IV International Forum (Generation IV International Forum, 2006). An abridged overview of these indicators, based on the aforementioned reference, with justification of the values used in this study, is presented below.

Table 12
Parameters used in calculating the levelised cost of electricity.

Parameter	Lower estimate	Middle estimate	Upper estimate	Distribution
Overnight capital construction cost ($/kWe) for EPR	3860[a]	6442[b]	9861[c]	Triangular
Fixed O&M costs ($/kWe.yr) for EPR[d]	45.00	56.25	67.50	Uniform
Variable O&M costs ($/kWh) for EPR[e]	0.23	0.27	0.30	Uniform
Decommissioning cost ($/kWe) for EPR[f]	644	805	966	Uniform
Overnight capital construction cost ($/kWe) for GT-MHR[g]	3818	5455	8180	Triangular
Fixed O&M costs ($/kWe.yr) for GT-MHR[g]	105	131	157	Uniform
Variable O&M costs ($/kWh) for GT-MHR[e]	0.23	0.27	0.30	Uniform
Decommissioning cost ($/kWe) for GT-MHR[g]	344	430	516	Uniform
Overnight capital construction cost ($/kWe) for AHWR[h]	4136	5910	8862	Triangular
Fixed O&M costs ($/kWe.yr) for AHWR[i]	45	101	157	Uniform
Variable O&M costs ($/kWh) for AHWR[e]	0.23	0.27	0.30	Uniform
Decommissioning cost ($/kWe) for AHWR[f]	591	739	887	Uniform

[a] Lower estimate for the EPR CAPEX cost assumed for Flamanville 3 in International Energy Agency (2010).
[b] Middle estimate for the EPR CAPEX cost taken from the estimate of one of the Hinkley Point C reactors (British Broadcasting Corporation, 2013).
[c] Upper estimate for the EPR CAPEX cost taken from "Option D" in Table 3 of Harris et al. (2012) for one of the Hinkley Point C reactors.
[d] Fixed O&M costs from NOAK Gen III PWR listed in Table A.10 of Mott McDonald (2010).
[e] Variable O&M costs from NOAK Gen III PWR listed in Table A.10 of Mott McDonald (2010). No other data available for other reactors.
[f] Decommissioning cost assumed to range between 10% and 15% of CAPEX costs.
[g] GT-MHR costs taken for a NOAK high temperature gas-cooled reactor (HTGR) from Idaho National Laboratory (2012). Upper and lower ranges of fixed O&M due to assumed to be 80% and 120% of middle value.
[h] Capital cost upscaled from GT-MHR estimate using the ratio of CAPEX costs in OECD-NEA (2011).
[i] No data for O&M costs exist. Therefore, lower value for EPR and upper value of GT-MHR assumed.

Table 13
Breakdown of the LCOE for the four nuclear fuel cycles under consideration, giving mean values (and uncertainties to one standard deviation). Reactor cost also accounts for decommissioning costs. Fuel cycle costs accounts for both front- and back-end costs and are values taken from Section 6.1.

Option	Levelised reactor cost ($/MWh)	Levelised O&M cost ($/MWh)	Levelised fuel cycle cost ($/MWh)	Levelised cost ($/MWh)
EPR with UO_2	88 ± 16	23 ± 3	10 ± 2	121 ± 16
EPR with UO_2/ThO_2	88 ± 16	23 ± 3	11 ± 3	122 ± 17
AHWR with UO_2/ThO_2	84 ± 13	41 ± 13	12 ± 2	137 ± 18
GT-MHR with UO_2/ThO_2	78 ± 12	53 ± 6	26 ± 5	157 ± 14

Table 14
Quantities of uranium heavy metal and its isotopic composition, per discharge, for the four nuclear energy systems. For the Th–U-fuelled EPR, the compositions of the seed [S] and blanket [B] assemblies are treated separately. For the Th–U-fuelled GT-MHR, the compositions of the once-irradiated driver fuel [DF] and twice-irradiated post-driver fuel [PDF] are treated separately.

Reactor	Quantities			Vector (%)						
	U_{TOT} (t)	^{235}U (kg)	^{233}U (kg)	^{232}U	^{233}U	^{234}U	^{235}U	^{236}U	^{237}U	^{238}U
EPR with UO_2	39.6	459	0.00	0.00	0.00	0.03	1.16	0.70	0.00	98.11
EPR [S] with UO_2	9.28	425	0.00	0.00	0.00	0.09	4.58	2.67	0.00	92.66
EPR [B] with UO_2/ThO_2	12.9	106	1440	0.09	11.21	2.80	0.83	1.35	0.00	83.72
AHWR with UO_2/ThO_2	0.97	22.5	57.9	0.06	5.94	0.93	2.31	3.35	0.00	87.42
GT-MHR [DF] with UO_2/ThO_2	1.16	179	15.4	0.00	1.33	0.05	15.50	1.20	0.00	81.92
GT-MHR [PDF] with UO_2/ThO_2	1.23	155	21.8	0.00	1.77	0.11	12.60	1.94	0.00	83.58

Table 15
As Table 14, but with quantities of plutonium heavy metal and its isotopic composition, per discharge, for the four nuclear energy systems.

Reactor	Quantities		Vector (%)				
	Pu_{TOT} (kg)	^{239}Pu (kg)	^{238}Pu	^{239}Pu	^{240}Pu	^{241}Pu	^{242}Pu
EPR with UO_2	516	275	2.41	53.27	23.47	14.66	6.19
EPR [S] with UO_2	217	117	6.49	53.74	15.31	17.82	6.64
EPR [B] with UO_2/ThO_2	462	211	9.61	45.73	13.41	17.23	14.02
AHWR with UO_2/ThO_2	14.2	5.97	9.33	41.88	21.72	14.62	12.44
GT-MHR [DF] with UO_2/ThO_2	23.6	18.7	0.35	79.31	11.22	8.51	0.61
GT-MHR [PDF] with UO_2/ThO_2	37.9	25.6	1.88	67.68	12.46	15.66	2.32

MT describes the material type on a five-point Likert scale. In decreasing desirability, the material types are: HEU [*MT* = 1], weapons-grade plutonium (WG-Pu) [*MT* = 2], reactor-grade plutonium (RG-Pu) [*MT* = 3], deep-burn plutonium (DB-Pu) [*MT* = 4], and LEU [*MT* = 5].

For plutonium: in Generation IV International Forum (2006), WG-Pu is ascribed as typically containing ~94% fissile plutonium content (i.e. ^{239}Pu and ^{241}Pu), RG-Pu as typically containing ~70% fissile plutonium content, and DB-Pu as typically containing ~43% fissile plutonium content. Other works also look at the isoto-

Table 16
Summary of the NNL proliferation resistance assessment methodology for the plutonium component of the SNF. The numbers in brackets denote the combined percentage of fissile ^{239}Pu and ^{241}Pu relative to all plutonium isotopes. N.B. A higher NNL *U(x)* score denotes a greater degree of proliferation resistance.

	EPR UO_2	EPR UO_2/ThO_2 [S]	EPR UO_2/ThO_2 [B]	AHWR UO_2/ThO_2	GT-MHR UO_2/ThO_2 [DF]	GT-MHR UO_2/ThO_2 [PDF]
SQs/GWy	29.3	19.0	8.3	6.6	25.0	40.2
Material Type [*MT*]	RG-Pu [3] (67.9%)	RG-Pu [3] (71.6%)	RG-Pu [3] (63.0%)	RG-Pu [3] (56.5%)	RG-Pu [3] (87.8%)	RG-Pu [3] (83.3%)
Technical Difficulty [*TD*]	Medium [3]	Medium [3]	High [4]	High [4]	High [4]	High [4]
Proliferation Cost [*PC*]	Medium [3]	Medium [3]	Medium [3]	Medium [3]	Medium [3]	Medium [3]
Proliferation Time [*PT*]	High [4]	High [4]	High [4]	High [4]	High [4]	High [4]
Detection Probability [*DP*]	High [4]	High [4]	Very High [5]	Very High [5]	High [4]	High [4]
NNL *U*(*x*)	7.03	7.22	8.58	8.68	6.60	6.40

Table 17
Summary of the NNL proliferation resistance methodology for the uranium component of the SNF. The numbers in brackets denote the ^{233}U equivalent percentage of fissile uranium, as described in Eq. (7). N.B. A higher NNL *U(x)* score denotes a greater degree of proliferation resistance.

	EPR UO_2	EPR UO_2/ThO_2 [S]	EPR UO_2/ThO_2 [B]	AHWR UO_2/ThO_2	GT-MHR UO_2/ThO_2 [DF]	GT-MHR UO_2/ThO_2 [PDF]
SQs/GWy (assuming LEU)	239.6	86.5	24.8	47.9	118	125
SQs/GWy (assuming ^{nat}U(eq))	1.80	0.65	0.19	0.36	0.89	0.94
Material Type [*MT*]	LEU [5] (0.70%)	LEU [5] (2.75%)	LEU [5] (11.7%)	LEU [5] (7.3%)	LEU [5] (10.6%)	LEU [5] (9.3%)
Technical Difficulty [*TD*]	High [4]	High [4]	Very High [5]	Very High [5]	High [4]	High [4]
Proliferation Cost [*PC*]	Medium [3]	Medium [3]	Medium [3]	Medium [3]	Medium [3]	Medium [3]
Proliferation Time [*PT*]	High [4]	High [4]	High [4]	High [4]	High [4]	High [4]
Detection Probability [*DP*]	High [4]	High [4]	Very High [5]	Very High [5]	High [4]	High [4]
NNL *U*(*x*) (assuming LEU)	7.58	8.06	9.61	9.32	7.93	7.90
NNL *U*(*x*) (assuming ^{nat}U(eq))	9.70	10.2	11.7	11.4	10.1	10.0

pic properties of plutonium grades: (1) Mark et al. (2009) gives typical values of 94.2% fissile plutonium content (inclusive of ^{241}Am) for WG-Pu, 69.4% RG-Pu (from U-based fuel, enriched to 3.0% ^{235}U with a discharge burn-up of 33 GWd/t), and spent "MOX-grade" fuel as 58.2% and (2) Kessler (2011) gives a range of plutonium vectors for WG-Pu, low burn-up fuels, high burn-up fuels and MOX-grade fuels. WG-Pu, very low burn-up fuel and U-based breeder blankets are listed as containing 88–96% fissile plutonium content. RG-Pu, derived from a number of reactors with discharge burn-ups of 5.0 GWd/t (for MAGNOX), 7.5 GWd/t (for CANDU), and 30, 50, 60, 72 GWd/t (for LWRs), provide a range of discharged fissile plutonium contents from 73.8% down to 64.7%. In both works, no mention of DB-Pu is made, although in Kessler, (2011), isotopics are provided for multiple-recycled MOX fuels which are considered "proliferation proof", and these have an upper limit of 44.7% fissile plutonium content.

For uranium: HEU is generally defined as uranium with a sufficiently large fissile fraction to constitute a nuclear explosive device. The weapons-grade uranium label is typically ascribed to uranium enriched to 95% ^{235}U (e.g. in Generation IV International Forum (2006)). It should be noted that the threshold between LEU and HEU is set at an enrichment threshold of 20% ^{235}U (International Atomic Energy Agency, 2002; Glaser, 2006). To account for ^{233}U isotopic content in fresh or spent nuclear fuel, it is suggested that a ^{233}U/^{238}U ratio of 12:88 would be considered as the threshold between LEU and HEU (cf. a ^{235}U/^{238}U ratio of 20:80) (Forsberg et al., 1998; Kang and von Hippel, 2001). Eq. (7), in which *M* is the mass of the given isotope(s), shows the redefined ^{233}U limit, accounting for the ^{235}U content (Forsberg et al., 1998). It should be noted that for freshly discharged fuel, the amount of ^{233}Pa would need to be added to the numerator and of all protactinium isotopes to the denominator.

$$\frac{M[^{233}U] + 0.6M[^{235}U]}{M[^{all}U]} \leqslant 0.12 \quad (7)$$

For the four nuclear fuel cycles considered here, each of the systems provide more than one SQ of plutonium. It should be noted that the fuel cycle modelling approach for the AHWR assumes that there is an annual discharge of fuel per year (totalling one tenth of the core). In practice, it is proposed that the refuelling scheme would be based around an "on-line" approach, and so each discharge could potentially be performed on a cluster-by-cluster approach. A significant question remains as to the variation of desirability of the plutonium in the SNF. In this analysis, it is assumed that the plutonium isotopic vectors of each nuclear fuel cycle (including seed/blanket assemblies and driver/post-driver blocks) correspond to RG-Pu [*MT* = 3]. For the discharged uranium, the question remains as to the potential for re-enrichment with and without separation by laser enrichment techniques. This significantly affects whether such material can be considered as LEU [*MT* = 5; 1 SQ = 75 kg] or equivalent to natural uranium (^{nat}U (eq)) [*MT* = 5; 1 SQ = 10,000 kg].

The remaining indicators (*TD*, *PC*, *PT*, *DP*) are described by qualitative descriptors in the form of five-point Likert scales with the scores: "very low" [1], "low" [2], "medium" [3], "high" [4], and "very high" [5]. There is the potential for more quantitative indicators (requiring analyses containing confidential/classified information) to be used. Given that this a comparative study that is limited to four open nuclear fuel cycles, and that analyses for some of the technologies using this methodology exist in UK National Nuclear Laboratory (2009), differences in the scoring of these components will be based on this previously published work.

TD corresponds to "technical difficulty" which, from a state perspective, could be considered as the probability of the proliferation pathway failing. From a nuclear fuel cycle perspective this can include material properties such as the spontaneous neutron emission rate, decay heat, radiotoxicity, and the material form. From UK National Nuclear Laboratory (2009) for a reference U-fuelled PWR (with discharge burn-up of 45 GWd/t), *TD* was described as "medium" [*TD* = 3]. For the plutonium component, *TD* is also described as medium for the reference U-fuelled EPR and the seed

assemblies of the Th–U-fuelled EPR. For the blanket assemblies of the Th–U-fuelled EPR and for the Th–U-fuelled AHWR, *TD* is classed as "high" [*TD* = 4] due to the enhanced content of ^{238}Pu, which provides additional complication to conventional aqueous-based reprocessing techniques, and the enhanced radiotoxicity associated with the decay of ^{232}U contained within the nuclear fuel. For the Th–U-fuelled GT-MHR, *TD* is ascribed as "high" [*TD* = 4] due to the additional process steps required to access the nuclear fuel kernels. In UK National Nuclear Laboratory (2009) *TD* for the HTGR is attributed as "very high" [*TD* = 5], this stronger classification being mainly due to the discharged material being equivalent to DB-Pu. For the uranium component, each of the values is increased by a single point on the Likert scale due to the additional re-enrichment step required, which, due to the content of ^{232}U and ^{234}U in some of the nuclear energy systems, may only be possible by using laser enrichment techniques.

PC corresponds to "proliferation cost" which could be described in terms of a country's military expenditure per year. As this study is not state-specific using a more pertinent metric would involve the differences within the infrastructure required. As only open nuclear fuel cycles are considered here, it is assumed that the reprocessing infrastructure required to generate a SQ of either plutonium or uranium, even including the additional process steps associated with the GT-MHR-based fuel, for each nuclear fuel cycle would be near identical. Therefore, for all fuel cycles *PC* is scored identically as "medium" [*PC* = 3].

PT corresponds to "proliferation time" which is described as the amount of time required to generate a SQ of material. Although reprocessing stages can potentially be performed covertly within a 3–12 month time frame (Generation IV International Forum, 2006), the time required to build up the infrastructure and expertise can take many years. In this analysis, the differences in reprocessing infrastructure required for the different fuel cycles under consideration are assumed to be negligible and therefore each cycle is scored identically as "high" [*PT* = 4].

DP corresponds to "detection probability" which is described as the probability that illicit movement of material is detected (in concordance with IAEA safeguards). From a fuel cycle perspective, this boils down to a series of factors including: the refuelling scheme, the size and composition of nuclear fuel assembly, the ability for non-safeguarded material to be irradiated, and the external radiation field. For the reference EPR this is considered as "high" [*DP* = 4] due to: (1) the large volume of the fuel assemblies; (2) the impossibility of on-line refuelling, and the length of time (over a year) between refuelling outages; (3) thermal–hydraulic instabilities from irradiating driver assemblies; and (4) the sizeable external radiation field due to the volume of material irradiated. These same factors are associated with the seed assemblies of the Th–U-fuelled EPR, while, for the blanket assemblies, *DP* is assessed as being "very high" [*DP* = 5] due to the presence of a sizeable ^{232}U component whose daughter product ^{208}Tl emits a 2.6 MeV γ ray that is difficult to shield. For the Th–U-fuelled AHWR, although the refuelling scheme is typically described as being "on-line", given that fuel can be continuously shuffled around the reactor, which lessens *DP*, this is offset by: (1) the low number of nuclear fuel clusters discharged per year; (2) the sizeable volume of each nuclear fuel cluster; and (3) the high ^{232}U content. Therefore *DP* is also attributed as being "very high". For the GT-MHR, due to the lower burn-up of the driver fuel, the smaller amounts of ^{232}U generated, and, most importantly, the fact that the 7.93 m nuclear fuel hexagonal block has to be separated into ten smaller blocks before being disposed of, *DP* for both driver and post-driver fuel is listed as "high" [*DP* = 4].

The results from this discussion are summarised in Table 16 for plutonium and Table 17 for uranium. In summary, although open-cycle U-fuelled PWRs can be considered highly resistant against proliferation, it is evident that there are small proliferation resistance advantages for the SNF discharged from the open-cycle Th–U-fuelled EPR and open-cycle Th–U-fuelled AHWR, due primarily to the lower amount of plutonium discharged per GWy. For the open-cycle Th–U-fuelled GT-MHR, the low discharge burn-up contributes towards a greater amount of plutonium being generated per GWy. For the Th–U-fuelled EPR, the limiting factor in terms of its proliferation resistance score comes from the discharged seed assemblies, although this score is higher than that of the U-fuelled EPR. For the AHWR, due to all the assemblies being comprised of blended UO_2/ThO_2, the proliferation resistance is comparably greater. It should be stressed that the overall proliferation score is on a qualitative non-linear scale. The benefits arising due to the nature of the SNF have to be set against the enhanced separative work capacity per kWh for these fuel cycles, the need for ^{235}U enriched to 20%, and the requirement of heavy water for the AHWR.

8. Conclusions

This paper has set out to compare a number of Th–U-fuelled nuclear energy systems operating with an open nuclear fuel cycle to a reference system. Reactor physics simulations were performed for one U-fuelled system (an AREVA EPR, which was treated as the reference) and three Th–U-fuelled systems (an AREVA EPR fuelled with a seed-blanket configuration, an Indian AHWR, and General Atomics' GT-MHR). Shielded reaction cross-sections from these simulations were then used by the NNL fuel cycle modelling code ORION to determine the front-end fuel cycle requirements (in terms of the uranium, thorium, and separative work capacity required) and characteristics of the back-end (in terms of the amount of spent fuel discharged, its isotopic composition and corresponding characteristics). These values have subsequently been used to assess the properties of the spent fuel, fuel cycle economics and its proliferation resistance.

In terms of the material flow, it is evident that although there is a smaller amount of uranium contained within the nuclear fuel, all of the Th–U-fuelled systems within this study, require more separative work units per kWh than the U-fuelled benchmark. This is predominantly due to the requirement of uranium enriched to ~20%. For the AHWR, ~6% less uranium ore (per kWh) is required than for the reference U-fuelled EPR. For the Th–U-fuelled EPR and Th–U-fuelled GT-MHR, more uranium ore is required than for the reference U-fuelled EPR. Although this is not an exhaustive study of all possible open cycle Th–U-fuelled nuclear energy systems, it is evident that significantly lower uranium enrichments are required for a notable advantage in resource utilisation to be realised in open cycles. Even if such designs can be realised, any advantage may not be significant enough to warrant a switch in fuelling options, particularly if the ratio of burn-up to uranium enrichment required for U-fuelled systems can be further enhanced. It should be stressed that the Th–U-fuelled GT-MHR needs further development and optimisation to ensure that there is greater utilisation of the nuclear fuel.

In terms of the spent fuel generated, the Th–U-fuelled EPR yields the smallest volume of SNF per kWh generated. This is principally due to the very long dwell times of blanket assemblies (~13.5 years). Correspondingly, the quantities of minor actinides within the discharged blanket assemblies are greater than for the U-fuelled seed assemblies. This could potentially complicate the encapsulation and long-term disposal. Overall, per kWh generated there are minimal differences in the decay heat and radiotoxicity of the fuel for each system considered.

In terms of the economics, the U-fuelled EPR has the lowest LFCC. This is predominantly due to the greater fuel fabrication

costs and additional separative work required by the Th–U-fuelled systems. In the analysis it is noted that the fuel fabrication costs for the Th–U-fuelled EPR seed and blanket fuel pins and the AHWR could be underestimated due to the need for novel fabrication techniques and variations in the ratio of UO_2 and ThO_2 required. Such variations are exemplified with the estimates for the GT-MHR fuel fabrication costs. In terms of the LCOE, although accurate estimates for capital and O&M are difficult to come by, we suggest that the U-fuelled EPR yields the lowest LCOE, on the assumption that the reactor is constructed in the West. We stress that this analysis should be treated only as indicative.

In terms of the proliferation resistance of the SNF, small advantages are observed for the Th–U-fuelled EPR and greater advantages are noted for the Th–U-fuelled AHWR. The low discharge burn-up of the GT-MHR design compromises its proliferation resistance score.

Overall, it appears that there is little merit in incorporating thorium into nuclear energy systems operating with *open nuclear fuel cycles*. In this study, three Th–U-fuelled reactor systems were considered. Two of these offer benefits in comparison to the reference U-fuelled system in terms of proliferation resistance, but this must be set against their need for uranium enriched to ~20% ^{235}U and thus more separative work capacity, with limited savings in uranium ore and waste generated, than for the U-fuelled reference. The economics also appear to favour the reference case. These downsides are in addition to various technical and licensing barriers for such reactors and fuel cycle infrastructures to be commissioned, as outlined in detail in Nelson (2012).

Acknowledgements

This work is supported by the UK Engineering and Physical Sciences Research Council under Grant No. EP/I018425/1. Two of the authors (SFA and WJN) would like to acknowledge the generous welcome provided by Bhabha Atomic Research Centre during a visit to their facilities.

References

AREVA, 2007. UK EPR Safety, Security and Environmental Report. Fundamental Safety Overview. Design and Safety, vol. 2. Chapter D: Reactor and core (v2). URL http://www.epr-reactor.co.uk/ssmod/liblocal/docs/V3/Volume%202%20-%20Design%20and%20Safety/2.D%20-%20Reactor%20and%20Core/2.D.1%20-%20Summary%20Description%20-%20v2.pdf (accessed 15.03.14).

AREVA, 2012. Pre-construction Environmental Report. Chapter 3: Aspects Having a Bearing on the Environment during Operation Phase. UKEPR-0003-030 Issue 5. <http://www.epr-reactor.co.uk/ssmod/liblocal/docs/PCER/Chapter%20%203%20-%20Aspects%20having%20a%20Bearing%20on%20the%20Environment%20during%20Operation%20Phase/Chapter%203%20-%20Aspects%20having%20a%20Bearing%20on%20the%20Environment%20during%20Operation%20Phase.pdf> (accessed 15.03.14).

Ashley, S.F., Nuttall, W.J., Parks, G.T., Worrall, A., 2012. On the proliferation resistance of thorium–uranium nuclear fuel. In: Proc. 2012 UK PONI Conference. <http://www.rusi.org/downloads/assets/UK_PONI_2012_-_Ashley_-_Prolfieration_Resistance_of_Thorium-Uranium_Fuel2.pdf> (accessed 15.03.14).

Ashley, S.F., Fenner, R.A., Nuttall, W.J., Parks, G.T., 2013. Open cycle thorium–uranium-fuelled nuclear energy systems. Proc. ICE Energy 166 (2), 74–81.

Benedict, M., Pigford, T.H., Levi, H.W., 1981. Nuclear Chemical Engineering, 2nd ed. McGraw-Hill, New York, ISBN: 978-0-070045316..

Bhabha Atomic Research Centre, 2012. AHWR300-LEU Advanced Heavy Water Reactor with LEU-Th MOX Fuel. <http://dae.nic.in/writereaddata/.pdf_31> (accessed 15.03.14).

Breismeister, J.F., (Ed.) 2000. MCNP – A General Monte Carlo n–Particle Transport Code, version 4C. Los Alamos National Laboratory Rep. LA–13709–M. <http://library.lanl.gov/cgi-bin/getfile?00818065.pdf> (accessed 15.03.14).

British Broadcasting Corporation, 2013. New Nuclear Power Plant at Hinkley Point C is Approved. <http://www.bbc.co.uk/news/uk-21839684> (accessed 15.03.14).

Cetnar, J., Wallenius, J., Gudowski, W., 1999. MCB: a continuous energy Monte Carlo burnup simulation code. In: Actinide and Fission Product Partitioning and Transmutation, vol. EUR 18898 EN. OECD/NEA Publ.

Cowper, M., 2012. Modelling the AHWR. M.Sc. Dissertation, University of Liverpool.

De Roo, G., Parsons, J.E., 2011a. A methodology for calculating the levelized cost of electricity in nuclear power systems with fuel recycling. Energy Econ. 33 (5), 826–839.

De Roo, G., Parsons, J.E., 2011b. Nuclear Fuel Recycling – The Value of the Separated Transuranics and the Levelized Cost of Electricity. Computer Code. <http://web.mit.edu/ceepr/www/publications/workingpapers/DeRooParsons_spreadsheet.xls> (accessed 15.03.14).

European Commission, Joint Research Centre, Institute for the Protection and Security of the Citizen, 2007. Computer Code: SimLab. <http://simlab.jrc.ec.europa.eu/> (accessed 15.03.14).

Forsberg, C.W., Hopper, C.M., Richter, J.L., Vantine, H.C., 1998. Definitions of Weapons-usable Uranium-233. Oak Ridge National Laboratory Rep. ORNL/TM-13517. <http://web.ornl.gov/info/reports/1998/3445606041609.pdf>.

General Atomics, 2002. Assessment of GT-MHR Spent Fuel Characteristics and Repository Performance. General Atomics Rep. PC-000502 Rev. 0. <https://inlportal.inl.gov/portal/server.pt/document/102615/assessment_of_gt-mhr_spent_fuel_characteristics_and_repository_performance_pdf>.

Generation IV International Forum, 2006. Evaluation Methodology for Proliferation Resistance and Physical Protection of Generation IV Nuclear Energy Systems. Rev. 5. Rep. GIF/PRPPWG/2006/005.

Glaser, A., 2006. On the proliferation potential of uranium fuel for research reactors at various enrichment levels. Sci. Glob. Sec. 14 (1), 1–24.

Gregg, R., Grove, C., 2012. Analysis of the UK nuclear fission roadmap using the ORION fuel cycle modelling code. In: Proc. IChemE Nuclear Fuel Cycle Conference. IChemE, Manchester, UK.

Hallstadius, L., Johnson, S., Lahoda, E., 2012. Cladding for high performance fuel. Prog. Nucl. Energy 57, 71–76.

Harris, G., Heptonstall, P., Gross, R., Handley, D., 2012. Cost Estimates for Nuclear Power in the UK. Working Paper ICEPT/WP/2012/014, Imperial College London.

Hesketh, K., 2012. A new non-proliferation assessment tool. Nucl. Eng. Int. 57 (697), 36–40, <http://www.neimagazine.com/features/featurea-new-non-proliferation-assessment-tool/> (accessed 15.03.14).

Hesketh, K.W., Worrall, A., 2010. Benchmarking UK National Nuclear Laboratory's proliferation resistance assessment methodology. Trans. Am. Nucl. Soc. 102, 122–123.

Idaho National Laboratory, 2012. Assessment of High Temperature Gas-cooled Reactor (HTGR) Capital and Operating Costs. Idaho National Laboratory Rep. TEV-1196 Rev. 1. <https://inlportal.inl.gov/portal/server.pt/document/101368/assessment_of_high_temperature_gas-cooled_reactor_-_htgr_-_capital_and_operating_costs_pdf> (accessed 15.03.14)

International Atomic Energy Agency, 2002. International Nuclear Verification Series No. 3: Safeguards Glossary 2001 Edition. ISBN: 92-0-111902-X. <http://www-pub.iaea.org/MTCD/publications/PDF/nvs-3-cd/PDF/NVS3_prn.pdf>.

International Atomic Energy Agency, 2012a. Communication Received from the Permanent Mission of the United States of America to the International Atomic Energy Agency Regarding Certain Member States' Guidelines for the Export of Nuclear Material, Equipment and Technology. Rep. INFCIRC/254/Rev.11/Part 1. <http://www.iaea.org/Publications/Documents/Infcircs/2012/infcirc254r11p1.pdf> (accessed 15.03.14).

International Atomic Energy Agency, 2012b. Role of Thorium to Supplement Fuel Cycles of Future Nuclear Energy Systems. Rep. NF-T-2.4. ISBN: 978-9-2-01259-103. <http://www-pub.iaea.org/MTCD/Publications/PDF/Pub1540_web.pdf>.

International Commission on Radiological Protection, 1996. Age Dependent Doses to the Members of the Public from Intake of Radionuclides – Part 5 Compilation of Ingestion and Inhalation Coefficients (Publication 72). Ann. ICRP 26 (1), 1–91. <http://www.sciencedirect.com/science/article/pii/S0146645300891927>.

International Energy Agency, 2010. Projected Costs of Generating Electricity, 2010 Edition. ISBN: 9789264084308.

Kamei, T., Hakami, S., 2011. Evaluation and implementation of thorium fuel cycle with LWR and MSR. Prog. Nucl. Energy 53 (7), 820–824.

Kang, J., von Hippel, F.N., 2001. U-232 and the proliferation-resistance of U-233 in spent fuel. Sci. Glob. Sec. 9, 1–32.

Kessler, G., 2011. Proliferation-proof Uranium/Plutonium Fuel Cycles: Safeguards and Non-proliferation. KIT Scientific Publishing, <http://www.ksp.kit.edu/download/1000021572> (accessed 15.03.14).

Lahoda, E.J., 2004. Costs for manufacturing thorium–uranium dioxide for light water reactors. Nucl. Tech. 147 (1), 102–112.

Lindley, B.A., Drera, S.S., Kelly, J.F., Ashley, S.F., Parks, G.T., 2013. An open-cycle RBWR concept utilizing LEU-Th seed-blanket fuel. In: Proc. ICAPP 2013. Korean Nuclear Society, Jeju Island, Korea.

Mark, J.C., von Hippel, F., Lyman, E., 2009. Explosive properties of reactor-grade plutonium. Sci. Glob. Secur. 17 (2–3), 170–185.

Massachusetts Institute of Technology, 2011. The Future of the Nuclear Fuel Cycle. <http://mitei.mit.edu/system/files/The_Nuclear_Fuel_Cycle-all.pdf> (accessed 15.03.14).

Mott McDonald, 2010. UK Electricity Generation Costs Update. <https://www.gov.uk/government/uploads/system/uploads/attachment_data/file/65716/71-uk-electricity-generation-costs-update-.pdf> (accessed 15.03.14).

Nelson, A.T., 2012. Thorium: not a near-term commercial nuclear fuel. Bull. Atom. Sci. 68 (5), 33–44.

Newton, T.D., Hutton, J.L., 2002. The next generation WIMS lattice code: WIMS 9. In: Proc. PHYSOR2002. American Nuclear Society, Seoul, South Korea.

Nuclear Decommissioning Authority, 2009. Generic Design Assessment: Summary of Disposability Assessment for Wastes and Spent Fuel Arising from Operation of the UK EPR. NDA Tech. Note 11261814. <http://www.nda.gov.uk/documents/

upload/TN-17548-Generic-Design-Assessment-Summary-of-Disposability-Assessment-for-Wastes-and-Spent-Fuel-arising-from-Operation-of-the-EPWR.pdf>.

OECD-NEA, 1994. The Economics of the Nuclear Fuel Cycle. OECD/NEA Rep. 386. <http://www.oecd-nea.org/html/ndd/reports/efc/EFC-complete.pdf> (accessed 15.03.14).

OECD-NEA, 2000. The JEF-2.2 Nuclear Data Library. JEFF Rep. 17. <http://www.oecd-nea.org/dbdata/nds_jefreports/jefreport-17/Table_of_content.pdf> (accessed 15.03.14).

OECD-NEA, 2011. Current Status, Technical Feasibility and Economics of Small Nuclear Reactors. <http://www.oecd-nea.org/ndd/reports/2011/current-status-small-reactors.pdf> (accessed 15.03.14).

OECD-NEA Report, 2012. Uranium 2011: Resources, Demand and Production.

Pelowitz, D.B. (Ed.), 2007. MCNPX User's Manual Version 2.6.0, Los Alamos National Laboratory Rep. LA-CP-07-1473.

Pelowitz, D.B. et al., 2011. MCNPX 2.7.0 Extensions, Los Alamos National Laboratory Rep. LA-UR-11-02295.

Powney, D.J., Newton, T.D., 2004. Overview of the WIMS 9 Resonance Treatment. ANSWERS/WIMS/TR.26 Issue 1, SERCO, Winfrith, United Kingdom.

Rhodes, J., Edenius, M., 2003. CASMO-4: A Fuel Assembly Burnup Program User's Manual. SSP-01/400 Rev. 3, Studsvik Scandpower Inc.

Romanello, V., Salvatores, M., Schwenk-Ferrero, A., Gabrielli, F., Vezzoni, B., Rineiski, A., Fazio, C., 2012. Sustainable nuclear fuel cycles and world regional issues. Sustain 4 (6), 1214–1238.

Sengler, G., Forêt, F., Schlosser, G., Lisdat, R., Stelletta, S., 1999. EPR core design. Nucl. Eng. Des. 187, 79–119.

Shropshire, D.E., Williams, K.A., Smith, J.D., Dixon, B.W., Dunzik-Gougar, M., Adams, R.D., Gombert, D., Carter, J.T., Schneider, E., Hebditch, D., 2009. Advanced Fuel Cycle Cost Basis (Rev. 2). Idaho National Laboratory Rep. INL/EXT-07-12107. <http://www.inl.gov/technicalpublications/Documents/4536700.pdf>.

Sinha, R.K., Kakodkar, A., 2006. Design and development of the AHWR – the Indian thorium fuelled innovative nuclear reactor. Nucl. Eng. Des. 236 (7–8), 683–700.

Svensk Kärnbränslehantering AB, 2010. Design, Production and Initial State of the Canister. Tech. Rep. TR-10-14. ISSN 1404-0344. <http://www.inl.gov/technicalpublications/Documents/4536700.pdf>.

Svensk Kärnbränslehantering AB, 2011. Environmental Impact Statement: Interim Storage, Encapsulation and Final Disposal of Spent Nuclear Fuel. ISBN: 978-91-978702-5-2. <http://www.skb.se/upload/publications/pdf/21014-MKB%20ENG%20webb%20150dpi.pdf>.

Talamo, A., Gudowski, W., 2005. Adapting the deep burn in-core fuel management strategy for the gas turbine – modular helium reactor to a uranium–thorium fuel. Ann. Nucl. Energy 32 (16), 1750–1781.

Thakur, A., Singh, B., Pushpam, N.P., Bharti, V., Kannan, U., Krishnani, P.D., Sinha, R.K., 2011. Fuel cycle flexibility in advanced heavy water reactor (AHWR) with the use of Th-LEU fuel. In: Proc. Canadian Nuclear Society International Conference on the Future of Heavy Water Reactors. Canadian Nuclear Society, Ontario, Canada.

Todosow, M., Kazimi, M., 2004. Optimization of Heterogeneous Utilization of Thorium in PWRs to Enhance Proliferation Resistance and Reduce Waste. MIT Rep. MIT-NFC-TR-065.

Tulsidas, H., 2011. World Resources of Thorium: The Th–U-REE-P-UNFC Linkages. Presentation from the IAEA Technical Meeting on World Thorium Resources. Thiruvananthapuram, India.

UK National Nuclear Laboratory, 2009. Benchmarking of NNL Proliferation Resistance Assessment Methodology. NNL Rep. (09) 10634.

United Nations, 2007. Indicators for Sustainable Development: Guidelines and Methodologies, 3rd ed. <http://sustainabledevelopment.un.org/content/documents/guidelines.pdf> (accessed 15.03.14).

U.S. DOE, 2002. Yucca Mountain Science and Engineering Report. Rev. 1. Rep. DOE/RW-0539-1. <http://energy.gov/sites/prod/files/edg/media/SER.PDF> (accessed 15.03.14).

World Nuclear Association, 2009. The Global Nuclear Fuel Market: Supply and Demand 2009–2030. ISBN: 0-946777-41-1.

World Nuclear Association, 2013. World Nuclear Power Reactors and Uranium Requirements. <http://world-nuclear.org/info/Facts-and-Figures/World-Nuclear-Power-Reactors-Archive/Reactor-Archive-January-2013/#.UanF9h2PxU> (accessed 15.03.14).